



# Nonlinear dynamic behavior analysis of an elastically restrained double-beam connected through a mass-spring system that is nonlinear

Yuhao Zhao · Jingtao Du · Yilin Chen · Yang Liu

Received: 18 October 2022 / Accepted: 17 February 2023 / Published online: 7 March 2023  
© The Author(s), under exclusive licence to Springer Nature B.V. 2023

**Abstract** Some complex engineering structures can be modeled as multiple beams connected through coupling elements. When the coupling element is elastic, it can be simplified as a mass-spring system. The existing studies mainly concentrated on the double-beam coupled through elastic connectors, where the connector is simplified as the equivalent linear stiffness element or linear mass-spring system. Furthermore, many researches ignore rotational boundary restraints in analyzing dynamic behavior of the double-beam connected through elastic connectors, limiting their engineering generality. Considering the above limitations, this study attempts to employ the cubic nonlinear stiffness in the coupling mass-spring system and study the potential application of the mass-spring system that is nonlinear on the vibration control of the double-beam system. Using the variational method and the generalized Hamiltonian method build the corresponding system's governing functions. Applying the Galerkin truncation method (GTM) obtains the dynamic behavior of the double-beam connected through a mass-spring system that is nonlinear. According to this study, the change of the mass-spring system that is nonlinear significantly influences the dynamic behavior of the double-

beam system, where the complex dynamic behavior occurs under certain parameters of the mass-spring system that is nonlinear. Suitable parameters of the mass-spring system that is nonlinear are good at the vibration suppression at the boundary of the vibration system. Furthermore, the mass-spring system that is nonlinear can change the characteristics of the double-beam system's kinetic energy transfer. For the vibration model established in this work, a quasi-periodic vibration state can be regarded as a sign of the occurrence of the targeted energy transfer of the double-beam connected through a mass-spring system that is nonlinear.

**Keywords** Nonlinear vibration · Double-beam structures · Mass-spring system that is nonlinear · Elastic boundary constraints

## 1 Introduction

The beam structure is an important component of many complex structures in various engineering branches, including architectural engineering, aerospace engineering, marine engineering, and others. Beam structures are inevitably subjected to the unwanted vibration introduced by the working environment or energy equipment. The unwanted vibration negatively affects the stability and safety of beam structures. To suppress complex structures' vibration,

---

Y. Zhao · J. Du · Y. Chen · Y. Liu (✉)  
College of Power and Energy Engineering, Harbin Engineering University, Harbin 150001, People's Republic of China  
e-mail: liuyangly91@hrbeu.edu.cn

deeply understanding the vibration characteristics of beam structures is indispensable.

Vibration characteristics of beam structures have been broadly studied. Kang and Kim [1] summarized the early studies related to Euler–Bernoulli and Timoshenko beams, where the general boundary constraints were considered as boundary conditions of such beam structures. As one of the common engineering techniques, vibration characteristics of beams with elastic boundaries was obtained through the Fourier series [2]. To strengthen the convenience and applicability of the Fourier series, the improved Fourier series was proposed [3, 4], where the derivative of such a Fourier series was continuous at the boundary. Vibration characteristics of various beam structures with general boundary constraints were easily gained by employing the corresponding Fourier series [5–10]. The corresponding studies suggest that the boundary-smoothed Fourier series is accurate and correct in predicting the vibration characteristics of elastically restrained beams.

Nowadays, scholars have attempted to utilize the beneficial influence of nonlinearity to control the vibration level of elastic structures. According to the installation form, the nonlinear stiffness can be applied as nonlinear supports or nonlinear oscillators in the vibration control of beam structures. For beams with supporting nonlinearities, Özhan and Pakdemirli [11] studied three-to-one internal resonances motivated by cubic nonlinearities. Ghayesh et al. [12, 13] investigated the nonlinear vibration of beams attached with cubic nonlinear stiffness. Wang and Fang [14] and Mao et al. [15] studied the vibration of beams attached with supporting nonlinearity. Tang et al. [16] exploited the phase closure principle to predict the nonlinear characteristics of beams with nonlinear boundaries. Ding et al. [17, 18] proposed an adjustable nonlinear isolator. Considering the engineering practice, Ding and Chen [19] employed the adjustable nonlinear isolator in a slightly curved beam and studied its vibration transmissibility. Zhao and Du [20] studied the dynamic behavior of a pre-pressure beam attached with supporting nonlinearities.

For beam structures with nonlinear oscillators, Georgiades and Vakakis [21] studied the dynamic responses of a linear beam attached to a nonlinear oscillator. Such a nonlinear oscillator is defined as the nonlinear energy sink (NES). Ahmadabadi and Khadem [22, 23] and Kani et al. [24] investigated

vibration control and energy harvesting of the beam by employing the NES. For beam structures with different boundaries, Parseh et al. [25] and Kani et al. [26] studied the robustness of NESs. Parseh et al. [27] studied the stable steady-state dynamic responses of a nonlinear beam structure attached with an NES. Chen et al. [28] exploited parallel NESs to suppress the vibration of beam structures under the shock load. Then, the nonlinear forced vibration control of beam structures with an attached NES or boundary nonlinear energy sinks was studied in Refs [29, 30]. The above investigations suggest that a suitable utilization of nonlinear stiffness is good for the vibration control of beams.

On some engineering occasions, complex structures such as double-layer bridges, propulsion systems, and others can be modeled as multiple beams connected via coupling elements. When the coupling element is elastic, it can be simplified as a mass-spring system. Especially in marine engineering, ship propulsion shafting systems typically consist of multiple slender shafts. When studying the transverse vibration of such a shafting system under low rotation speed, such a slender shafting system can be simplified as beams connected through some coupling device, where the coupling device can be simplified as a mass-spring system. Furthermore, the axial motion of the shaft system is harmful to the stability of the shafting systems. Some limiters are installed on the shafting systems at both internal and boundary to limit their axial motion. For the simplified double-beam structures, Oniszczuk [31] investigated the free vibration of the double beams connected through a layer that is elastic. Gurgoze et al. [32] and Pajand and Hozhabrossadati [33] studied the bending vibration characteristics of double beams connected through a mass-spring system that was linear. Hilal [34] investigated the influence of a moving load on the dynamic responses of a double-beam system. Li and Hua [35] proposed a spectral finite element-based normal mode method to predict dynamic responses of the elastically connected double-beam. Rosa and Lippiello [36] established the vibration analysis model of the double-beam system joined by a Winkler-type soil, where free vibration of such a structure with generally restrained boundaries was studied. Zhang et al. [37], Stojanovic et al. [38], and Kozic et al. [39] investigated the vibration and buckling characteristics of a pre-pressure double-beam. Palmeri and Adhikari [40]

proposed a novel state-space form to predict dynamic responses of the double-beam structure joined by an inner viscoelastic layer. Mao [41, 42] employed the Adomian modified decomposition method to study the multiple-beam structure’s vibration characteristics and forced dynamic responses. Mohammadi and Nasirshoabi [43] studied forced dynamic responses of an elastically connected pre-pressure double-beam system with a Pasternak middle layer, where the double-beam structure was simply supported. Pisarski et al. [44] employed multiple smart damping members to suppress the vibration of the double-beam system. Fei et al. [45] proposed a new method to predict the vibration characteristics of a tensioned structure. Agboola et al. [46] studied the influence of structural parameters on the vibration characteristics of the double-beam, where the double-beam is non-prismatic and simply supported. Rahman and Lee [47] proposed a new modified multi-level residue harmonic balance method to predict nonlinear dynamic responses of a double-beam structure. Lee and Wang [48] investigated the transverse vibration of a double-beam system connected through coupling elements in experiments and theory, where the external force was non-uniform. Chen et al. [49], Hao et al. [50], Zhao and Asce [51], and Li et al. [52] studied vibration characteristics of double beams with classical and generally restrained boundary conditions. Pajand et al. [53] first considered the double beams connected through a three-degree-of-freedom system. Then, natural frequencies and mode shapes were predicted through a finite element method. Guo et al. [54] established the vibration analysis model of an asymptotically reduced coupled model, which was consisting of two inclined cables and one deck beam. The dynamic responses, stability, and bifurcations of such a vibration system were systematically investigated. Stojanovic et al. [55] investigated nonlinear vibrations and vibration transmissibility of a coupled beam-arch bridge system, where the coupling devices presented nonlinear characteristics and the bridge was geometrically nonlinear. According to the above references, the existing studies mainly concentrated on the double-beam coupled through elastic connectors, where the connector is simplified as the equivalent linear stiffness element or linear mass-spring system. Many researches ignore rotational boundary restraints in analyzing dynamic behavior of the double-beam

connected through elastic connectors, limiting their engineering generality.

Considering the above limitations and engineering practice, this study attempts to employ the cubic nonlinear stiffness in the coupling mass-spring system and study the potential application of the mass-spring system that is nonlinear on the transverse vibration of an elastically restrained double-beam system, where the axial motion of the double-beam system is ignored. Using the variational method and the generalized Hamiltonian method, the governing functions for a double-beam connected through a mass-spring system that is nonlinear are built. Applying the Galerkin truncation method (GTM) obtains the dynamic behavior of the double-beam connected through a mass-spring system that is nonlinear. The influence of the mass-spring system that is nonlinear on the transverse vibration of an elastically restrained double-beam system is researched.

## 2 Theoretical Formulations

### 2.1 Model Description

As illustrated in Fig. 1, the physical model of a double-beam connected through a mass-spring system that is nonlinear is built. Such a vibration system consists of two beams and a mass-spring system that is nonlinear.  $u_1(x_1, t)$ ,  $u_2(x_2, t)$ , and  $u_E(t)$  are vibration displacements of each beam and the mass-spring system that is nonlinear.  $E_1, E_2, \rho_1, \rho_2, S_1, S_2, I_1, I_2, C_{B1}$ , and  $C_{B2}$  are the elastic modulus, mass density, section area, inertia moment, and external viscous damping of each beam, respectively. To improve the generality of the vibration analysis model, this work studies the dynamic behavior of a double-beam

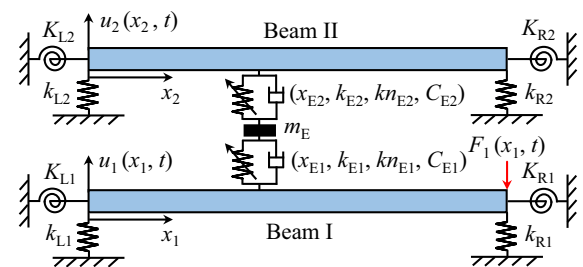


**Fig. 1** The physical model of a double-beam connected through a mass-spring system that is nonlinear

connected through a mass-spring system that is nonlinear with general boundary conditions. Boundary translational and rotational restraining springs are introduced at the boundary of each beam, where  $k_{L1}$ ,  $k_{L2}$ ,  $k_{R1}$ ,  $k_{R2}$ ,  $K_{L1}$ ,  $K_{L2}$ ,  $K_{R1}$ , and  $K_{R2}$  are stiffness coefficients of each boundary restraining spring. Different boundary conditions (clamped boundary, free boundary, simply support boundary, and elastic boundary) can be simulated by setting the stiffness coefficients of boundary restraining springs.  $k_{E1}$ ,  $k_{E2}$ ,  $kn_{E1}$ ,  $kn_{E2}$ ,  $C_{E1}$ ,  $C_{E2}$ , and  $m_E$  are the linear stiffness, nonlinear stiffness, viscous damping, and concentrated mass of the mass-spring system that is nonlinear.  $x_{E1}$  and  $x_{E2}$  are the positions of the mass-spring system that is nonlinear, where  $x_{E1}$  is the position of the system located at Beam I and  $x_{E2}$  is the position of the system located at Beam II. For this study, the nonlinear stiffness of the mass-spring system that is nonlinear is regarded as cubic stiffness, which can be realized through mechanism design.

In marine engineering, the shafting system under low rotation speed can be simplified as the double-beam system, where the external excitation introduced by the energy equipment typically locates on the determined position of the shafting system. In the vibration analysis, the corresponding external excitation can be approximated as a point excitation. Obviously, to ensure the service life of the energy equipment, the energy equipment is usually operated at its rated condition, which indicates that the external excitation introduced to shafting systems is typically periodic. Considering the above engineering situation, the point harmonic excitation is selected as the external excitation in this study.  $F_1(x_1, t)$  is the external force subjected to Beam I and its specific expression is defined as

$$F_1(x_1, t) = \delta(x_1 - L_1)F_1 \sin(\omega t) \tag{1}$$

where  $F_1$  is the amplitude of the excitation force,  $\delta(\cdot)$  is the Dirac function, and  $\omega$  is the circular frequency of the external excitation force.

Each beam in Fig. 1 is modeled as the Euler–Bernoulli beam. The potential energy and kinetic energy of the vibration system are derived as

$$V = V_{BeamI} + V_{BeamII} + V_{BoundaryI} + V_{BoundaryII} + V_E \tag{2a}$$

and

$$T = T_I + T_{II} + T_E \tag{2b}$$

$V_{BeamI}$  and  $V_{BeamII}$  are the potential energy of each beam.  $V_{BI}$  and  $V_{BII}$  are the potential energy of boundary restraining springs belonging to each beam.  $V_E$  is the potential energy of the mass-spring system that is nonlinear.  $T_I$ ,  $T_{II}$ , and  $T_E$  are the kinetic energy of each beam and the mass-spring system that is nonlinear.

The virtual work done by the external excitation force is derived as

$$\delta W_F = \delta W_{F1} \tag{3}$$

$\delta W_{F1}$  is the virtual work done by the external excitation force on Beam I.

The virtual work done by the viscous damping is derived as

$$\delta W_C = \delta W_{C1} + \delta W_{C2} + \delta W_{CE1} + \delta W_{CE2} \tag{4}$$

$\delta W_{C1}$  and  $\delta W_{C2}$  are the virtual work done by the viscous damping of Beam I and Beam II.  $\delta W_{CE1}$  and  $\delta W_{CE2}$  are the virtual work done by the viscous damping of the mass-spring system that is nonlinear. The specific form of each term of Eqs. (2), (3), and (4) are listed in Appendix A.

Using the variational method and the generalized Hamiltonian method, we can find the governing functions for a double-beam connected through a mass-spring system that is nonlinear, namely,

$$\begin{aligned} &\rho_1 S_1 \frac{\partial^2 u_1}{\partial t^2} + C_{B1} \frac{\partial u_1}{\partial t} + E_1 I_1 \frac{\partial^4 u_1}{\partial x_1^4} + F_1(x_{F1}, t) + \delta(x_1 - x_{E1}) \\ &\left\{ k_{E1}[u_1 - u_E(t)] + kn_{E1}[u_1 - u_E(t)]^3 + C_{E1} \left[ \frac{\partial u_1}{\partial t} - \frac{du_E(t)}{dt} \right] \right\} = 0 \end{aligned} \tag{5a}$$

$$\begin{aligned} &\rho_2 S_2 \frac{\partial^2 u_2}{\partial t^2} + C_{B2} \frac{\partial u_2}{\partial t} + E_2 I_2 \frac{\partial^4 u_2}{\partial x_2^4} + \delta(x_2 - x_{E2}) \\ &\left\{ k_{E2}[u_2 - u_E(t)] + kn_{E2}[u_2 - u_E(t)]^3 + C_{E2} \left[ \frac{\partial u_2}{\partial t} - \frac{du_E(t)}{dt} \right] \right\} = 0 \end{aligned} \tag{5b}$$

and

$$\begin{aligned} &m \frac{d^2 u_E}{dt^2} + C_{E1} \left[ \frac{du_E}{dt} - \frac{\partial u_1(x_{E1}, t)}{\partial t} \right] + C_{E2} \left[ \frac{du_E}{dt} - \frac{\partial u_2(x_{E2}, t)}{\partial t} \right] \\ &\quad + k_{E1}[u_E - u_1(x_{E1}, t)] + k_{E2}[u_E - u_2(x_{E2}, t)] \\ &\quad + kn_{E1}[u_E - u_1(x_{E1}, t)]^3 + kn_{E2}[u_E - u_2(x_{E2}, t)]^3 = 0 \end{aligned} \tag{5c}$$

Boundary conditions of the double-beam system are derived as

$$x_1 = 0: \quad k_{L1}u_1 + E_1I_1 \frac{\partial^3 u_1}{\partial x_1^3} = 0, \quad K_{L1} \frac{\partial u_1}{\partial x_1} - E_1I_1 \frac{\partial^2 u_1}{\partial x_1^2} = 0 \tag{6a}$$

$$x_1 = L_1: \quad k_{R1}u_1 - E_1I_1 \frac{\partial^3 u_1}{\partial x_1^3} = 0, \quad K_{R1} \frac{\partial u_1}{\partial x_1} + E_1I_1 \frac{\partial^2 u_1}{\partial x_1^2} = 0. \tag{6b}$$

$$x_2 = 0: \quad k_{L2}u_2 + E_2I_2 \frac{\partial^3 u_2}{\partial x_2^3} = 0, \quad K_{L2} \frac{\partial u_2}{\partial x_2} - E_2I_2 \frac{\partial^2 u_2}{\partial x_2^2} = 0 \tag{6c}$$

and

$$x_2 = L_2: \quad k_{R2}u_2 - E_2I_2 \frac{\partial^3 u_2}{\partial x_2^3} = 0, \quad K_{R2} \frac{\partial u_2}{\partial x_2} + E_2I_2 \frac{\partial^2 u_2}{\partial x_2^2} = 0. \tag{6d}$$

According to Eqs. (5a) and (5b), the nonlinear restoring force introduced to Beam I and Beam II can be defined as,

$$F_{N1} = \delta(x_1 - x_{E1})kn_{E1}[u_1 - u_E(t)]^3 \tag{7a}$$

and

$$F_{N2} = \delta(x_2 - x_{E2})kn_{E2}[u_2 - u_E(t)]^3 \tag{7b}$$

where  $F_{N1}$  is the nonlinear restoring force subjected to Beam I and  $F_{N2}$  is the nonlinear restoring force

subjected to Beam II. Furthermore, for the mass-spring system that is nonlinear, its nonlinear restoring force ( $F_{NE}$ ) can be fined as,

$$F_{NE} = kn_{E1}[u_E - u_1(x_{E1}, t)]^3 + kn_{E2}[u_E - u_2(x_{E2}, t)]^3 \tag{7c}$$

For the physical model established in this study, the corresponding terms of the generalized Hamiltonian principle are listed in Appendix B.

### 2.2 Solution Procedure

The governing functions of the vibration system derived in Sect. 2.1 are solved by the GTM. In this study, transverse vibration displacements of each beam are expanded as

$$u_1(x_1, t) = \sum_{i=1}^{N_1} \varphi_{1i}(x_1)q_{1i}(t) \tag{8a}$$

and

$$u_2(x_2, t) = \sum_{i=1}^{N_2} \varphi_{2i}(x_2)q_{2i}(t) \tag{8b}$$

where  $\varphi_{1i}(x_1)$  is the  $i$ th trial function of Beam I and  $\varphi_{2i}(x_2)$  is the  $i$ th trial function of Beam II.  $q_{1i}(t)$  and  $q_{2i}(t)$  are the  $i$ th unknown time terms of each beam.

After substituting Eq. (8) into Eqs. (5a) and (5b), the Galerkin discretization procedure is utilized to deal with the governing functions of each beam, namely,

$$\int_0^{L_1} \left\{ \begin{array}{l} \rho_1 S_1 \frac{\partial^2 u_1}{\partial t^2} + C_{B1} \frac{\partial u_1}{\partial t} + E_1 I_1 \frac{\partial^4 u_1}{\partial x_1^4} + F_1(x_1, t) \\ + \delta(x_1 - x_{E1}) \left\{ \begin{array}{l} k_{E1}[u_1 - u_E(t)] + kn_{E1}[u_1 - u_E(t)]^3 \\ + C_{E1} \left[ \frac{\partial u_1}{\partial t} - \frac{du_E(t)}{dt} \right] \end{array} \right\} \end{array} \right\} \psi_{1m_1}(x_1) dx_1 = 0 \tag{9a}$$

and

$$\int_0^{L_2} \left\{ \begin{array}{l} \rho_2 S_2 \frac{\partial^2 u_2}{\partial t^2} + C_{B2} \frac{\partial u_2}{\partial t} + E_2 I_2 \frac{\partial^4 u_2}{\partial x_2^4} \\ + \delta(x_2 - x_{E2}) \left\{ \begin{array}{l} k_{E2}[u_2 - u_E(t)] + kn_{E2}[u_2 - u_E(t)]^3 \\ + C_{E2} \left[ \frac{\partial u_2}{\partial t} - \frac{du_E(t)}{dt} \right] \end{array} \right\} \end{array} \right\} \psi_{2m_2}(x_2) dx_2 = 0 \tag{9b}$$

where  $\psi_{1i}(x_1)$  is the  $i$ th weight function of Beam I and  $\psi_{2i}(x_2)$  is the  $i$ th weight function of Beam II.  $m_1 = 1, 2, \dots, M_1$  and  $m_2 = 1, 2, \dots, M_2$ . Equation (9a) is the  $m_1$ th residual function of Beam I, and Eq. (9b) is the  $m_2$ th residual function of Beam II.

In the GTM, a set of functions that satisfy boundary conditions can be chosen as the trail and weight functions. For the physical model established in Sect. 3.1, mode functions of the elastically restrained single beam without the mass-spring system that is nonlinear exactly satisfy the corresponding boundary conditions. Therefore, the corresponding mode functions are chosen as the trail and weight functions. Such mode functions can be accurately obtained by employing the energy principle combined with the boundary-smoothed Fourier series [8–10].

Equation (9) is simplified as follows,

$$RI_{m_1 1} + RI_{m_1 2} + RI_{m_1 3} + RI_{m_1 4} + RI_{m_1 5} + RI_{m_1 6} + RI_{m_1 7} = 0 \tag{10a}$$

and

$$RII_{m_2 1} + RII_{m_2 2} + RII_{m_2 3} + RII_{m_2 4} + RII_{m_2 5} + RII_{m_2 6} = 0 \tag{10b}$$

The specific form of each residual term in Eq. (10) is listed in Appendix C.

To establish the matrix form of Eq. (10), Eq. (10) is transformed as

$$RI_{m_1 1} = -(RI_{m_1 2} + RI_{m_1 3} + RI_{m_1 4} + RI_{m_1 5} + RI_{m_1 6} + RI_{m_1 7}) \tag{11a}$$

and

$$RII_{m_2 1} = -(RII_{m_2 2} + RII_{m_2 3} + RII_{m_2 4} + RII_{m_2 5} + RII_{m_2 6}) \tag{11b}$$

The specific form of  $RI_{m_1 1}$  and  $RII_{m_2 1}$  is expanded as

$$RI_{m_1 1} = CI_{m_1 1} \frac{d^2 q_{11}}{dt^2} + CI_{m_1 2} \frac{d^2 q_{12}}{dt^2} + \dots + CI_{m_1 i} \frac{d^2 q_{1i}}{dt^2} + \dots + CI_{m_1 N_1} \frac{d^2 q_{1N_1}}{dt^2} \tag{12a}$$

and

$$RII_{m_2 1} = CII_{m_2 1} \frac{d^2 q_{21}}{dt^2} + CII_{m_2 2} \frac{d^2 q_{22}}{dt^2} + \dots + CII_{m_2 i} \frac{d^2 q_{2i}}{dt^2} + \dots + CII_{m_2 N_2} \frac{d^2 q_{2N_2}}{dt^2} \tag{12b}$$

Substituting Eq. (12) into Eq. (11), the specific form of Eq. (11) is derived as

$$CI_{m_1 1} \frac{d^2 q_{11}}{dt^2} + CI_{m_1 2} \frac{d^2 q_{12}}{dt^2} + \dots + CI_{m_1 i} \frac{d^2 q_{1i}}{dt^2} + \dots + CI_{m_1 N_1} \frac{d^2 q_{1N_1}}{dt^2} = - \sum_{i=2}^7 RI_{m_1 i} \tag{13a}$$

and

$$CII_{m_2 1} \frac{d^2 q_{21}}{dt^2} + CII_{m_2 2} \frac{d^2 q_{22}}{dt^2} + \dots + CII_{m_2 i} \frac{d^2 q_{2i}}{dt^2} + \dots + CII_{m_2 N_2} \frac{d^2 q_{2N_2}}{dt^2} = - \sum_{i=2}^6 RII_{m_2 i} \tag{13b}$$

Then, the matrix form of the residual functions is written as

$$\begin{bmatrix} CI_{11} & \dots & CI_{1i} & \dots & CI_{1N_1} \\ \dots & \dots & \dots & \dots & \dots \\ CI_{m_1 1} & \dots & CI_{m_1 i} & \dots & CI_{m_1 N_1} \\ \dots & \dots & \dots & \dots & \dots \\ CI_{M_1 1} & \dots & CI_{M_1 i} & \dots & CI_{M_1 N_1} \end{bmatrix} \begin{bmatrix} \frac{d^2 q_{11}}{dt^2} \\ \dots \\ \frac{d^2 q_{1i}}{dt^2} \\ \dots \\ \frac{d^2 q_{1N_1}}{dt^2} \end{bmatrix} = - \begin{bmatrix} \sum_{i=2}^7 RI_{1i} \\ \dots \\ \sum_{i=2}^7 RI_{m_1 i} \\ \dots \\ \sum_{i=2}^7 RI_{M_1 i} \end{bmatrix} \tag{14a}$$

and

$$\begin{aligned}
 & \begin{bmatrix} CII_{11} & \dots & CII_{1i} & \dots & CII_{1N_2} \\ \dots & \dots & \dots & \dots & \dots \\ CII_{m_21} & \dots & CII_{m_2i} & \dots & CII_{m_2N_2} \\ \dots & \dots & \dots & \dots & \dots \\ CI_{M_21} & \dots & CII_{M_2i} & \dots & CII_{M_2N_2} \end{bmatrix} \begin{bmatrix} \frac{d^2 q_{21}}{dt^2} \\ \dots \\ \frac{d^2 q_{2i}}{dt^2} \\ \dots \\ \frac{d^2 q_{2N_2}}{dt^2} \end{bmatrix} \\
 &= - \begin{bmatrix} \sum_{i=2}^6 RII_{1i} \\ \dots \\ \sum_{i=2}^6 RII_{m_2i} \\ \dots \\ \sum_{i=2}^6 RII_{M_2i} \end{bmatrix}.
 \end{aligned} \tag{14b}$$

Substituting Eq. (8) into Eq. (5c), the specific form of the governing function of the mass-spring system that is nonlinear is derived as

$$\begin{aligned}
 & m_E \frac{d^2 u_E}{dt^2} + C_{E1} \left[ \frac{du_E}{dt} - \sum_{i=1}^{N_1} \varphi_{1i}(x_{E1}) \frac{dq_{1i}(t)}{dt} \right] \\
 & + C_{E2} \left[ \frac{du_E}{dt} - \sum_{i=1}^{N_2} \varphi_{2i}(x_{E2}) \frac{dq_{2i}(t)}{dt} \right] \\
 & + k_{E1} \left[ u_E - \sum_{i=1}^{N_1} \varphi_{1i}(x_{E1}) q_{1i}(t) \right] \\
 & + k_{E2} \left[ u_E - \sum_{i=1}^{N_2} \varphi_{2i}(x_{E2}) q_{2i}(t) \right] \\
 & + kn_{E1} \left[ u_E - \sum_{i=1}^{N_1} \varphi_{1i}(x_{E1}) q_{1i}(t) \right]^3 \\
 & + kn_{E2} \left[ u_E - \sum_{i=1}^{N_2} \varphi_{2i}(x_{E2}) q_{2i}(t) \right]^3 = 0
 \end{aligned} \tag{15}$$

Equations (14a), (14b), and (15) compose the residual functions of the elastically restrained double-beam connected through a mass-spring system that is nonlinear. Such residual functions can be solved by numerical methods. By substituting the numerical results of Eqs. (14a), (14b), and (15) into Eq. (8), dynamic responses at arbitrary positions of the elastically restrained double-beam connected through a mass-spring system that is nonlinear can be gained. In the GTM, when the boundary condition changes, the dynamic behavior of the double-beam connected through a mass-spring system that is nonlinear under the changed boundary can be obtained conveniently

by changing the boundary restraining springs' stiffness coefficient. Furthermore, by introducing multiple nonlinear mass-spring systems in the double-beam system, the vibration analysis model established in this section can be extended to predict the dynamic behavior of the double-beam connected through multiple nonlinear mass-spring systems.

### 3 Simulation results and discussion

In this section, the correctness and stability of the GTM in solving the residual functions are studied first. Then, the influence of the mass-spring system that is nonlinear on dynamic responses of the double-beam is investigated. Furthermore, to improve the engineering acceptance of the mass-spring system that is nonlinear, in analyzing dynamic responses of the double-beam system with the variation of nonlinear mass-spring system's parameters, synchronous change parameters of the mass-spring system that is nonlinear.

With the prosperous study of the material field, lightweight and high-strength materials are gradually employed in engineering to alternative traditional materials. Therefore, this study investigates the potential application of the mass-spring system that is nonlinear for the double-beam system which is manufactured by aluminum alloy. Table 1 shows the structural parameters of the double-beam system. Table 2 gives the parameters of the mass-spring system that is nonlinear. Figure 2 presents the relation between the nonlinear restoring force and displacement of Beam I and Beam II, where  $u_1$ ,  $u_2$ , and  $u_E$  change from  $-0.02$  to  $0.02$  m. It can be seen from Fig. 2 that the nonlinear restoring force presents nonlinearity with the variation of  $u_1$ ,  $u_2$ , and  $u_E$ .

#### 3.1 Validation of the dynamic responses

This section investigates the correctness and stability of the GTM in solving the residual functions established in Sect. 2. The time-domain calculation range is selected as  $0 \sim 500 T_e$ , in which  $T_e$  is the period of the external excitation force, namely,

$$T_e = \frac{2\pi}{\omega} \tag{16}$$

$401 \sim 500 T_e$  is chosen as the stable calculation results of the double-beam connected through a mass-

**Table 1** Structural parameters of beams employed in the simulation

Parameters	Symbol (Unit)	Value
Elastic modulus	$E_1/E_2$ (Pa)	$6.89 \times 10^{10}/6.89 \times 10^{10}$
Mass density	$\rho_1/\rho_2$ (kg/m <sup>3</sup> )	$2.8 \times 10^3/2.8 \times 10^3$
Length	$L_1/L_2$ (m)	1/1
Section area	$S_1/S_2$ (m <sup>2</sup> )	$2 \times 10^{-4}/2 \times 10^{-4}$
Inertia moment	$I_1/I_2$ (m <sup>4</sup> )	$1.677 \times 10^{-9}/1.677 \times 10^{-9}$
Viscous damping	$C_{B1}/C_{B2}$ (Ns/m)	5/5
The amplitude of the excitation	$F_1 = 10$ (N)	10
Boundary translational stiffness	$k_{L1}/k_{L2}/k_{R1}/k_{R2}$ (N/m)	$5 \times 10^3/5 \times 10^3/5 \times 10^3 \times 10^3$
Boundary rotational stiffness	$K_{L1}/K_{L2}/K_{R1}/K_{R2}$ (Nm/rad)	$10^3/10^3/10^3/10^3$

**Table 2** Parameters of the mass-spring system that is nonlinear employed in numerical simulation

Parameters	Symbol (Unit)	Value
Concentrated mass	$m_E$ (kg)	0.02
Position	$x_{E1}/x_{E2}$ (m)	0.7/0.7
Viscous damping	$C_{E1}/C_{E2}$ (Ns/m)	5/5
Linear stiffness	$k_{E1}/k_{E2}$ (N/m)	$10^3/10^3$
Nonlinear stiffness	$kn_{E1}/kn_{E2}$ (N/m <sup>3</sup> )	$10^9/10^9$

spring system that is nonlinear. In the above time-domain region, transient dynamic responses of the vibration system have died away. The relation of the truncation number is set as  $N_1 = N_2 = M_1 = M_2$ . In plotting amplitude-frequency response curves of the double-beam connected through a mass-spring system that is nonlinear, the maximum value of the time-domain responses of the double-beam system under

each excitation frequency is selected as the y coordinate while the excitation frequency is selected as the x coordinate.

Firstly, the harmonic balance method (HBM) and Lagrange method (LM) are employed to verify the correctness of the GTM in obtaining the dynamic behavior of the double-beam connected through a mass-spring system that is nonlinear, where a 4-term truncation number is applied in this part. For HBM, the time terms are set as fundamental harmonics. For LM, the matrix equation of the double-beam connected through a mass-spring system that is nonlinear is established by employing the Lagrange function combined with the energy principle. It is worth mentioning that the GTM and LM are quite different in establishing the matrix equation of the double-beam system. Furthermore, the GTM and LM calculate the dynamic behavior of the double-beam system from the time domain while the HBM calculates it from the frequency domain. Figure 3 presents amplitude-

**Fig. 2** The relation between the nonlinear restoring force and displacement of Beam I and Beam II

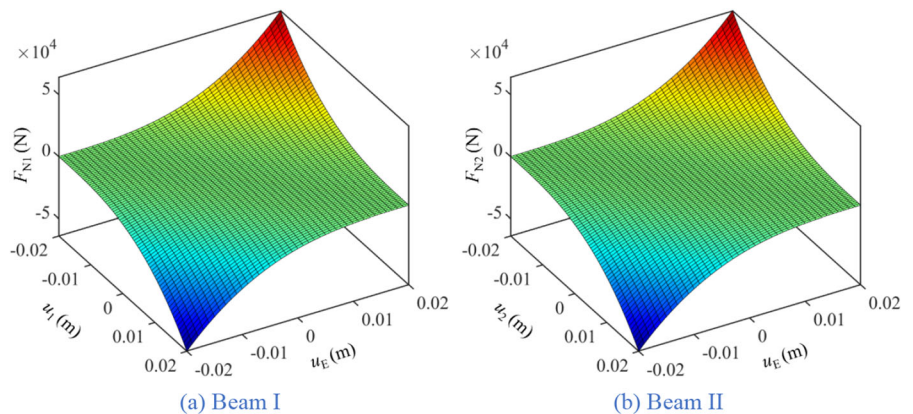
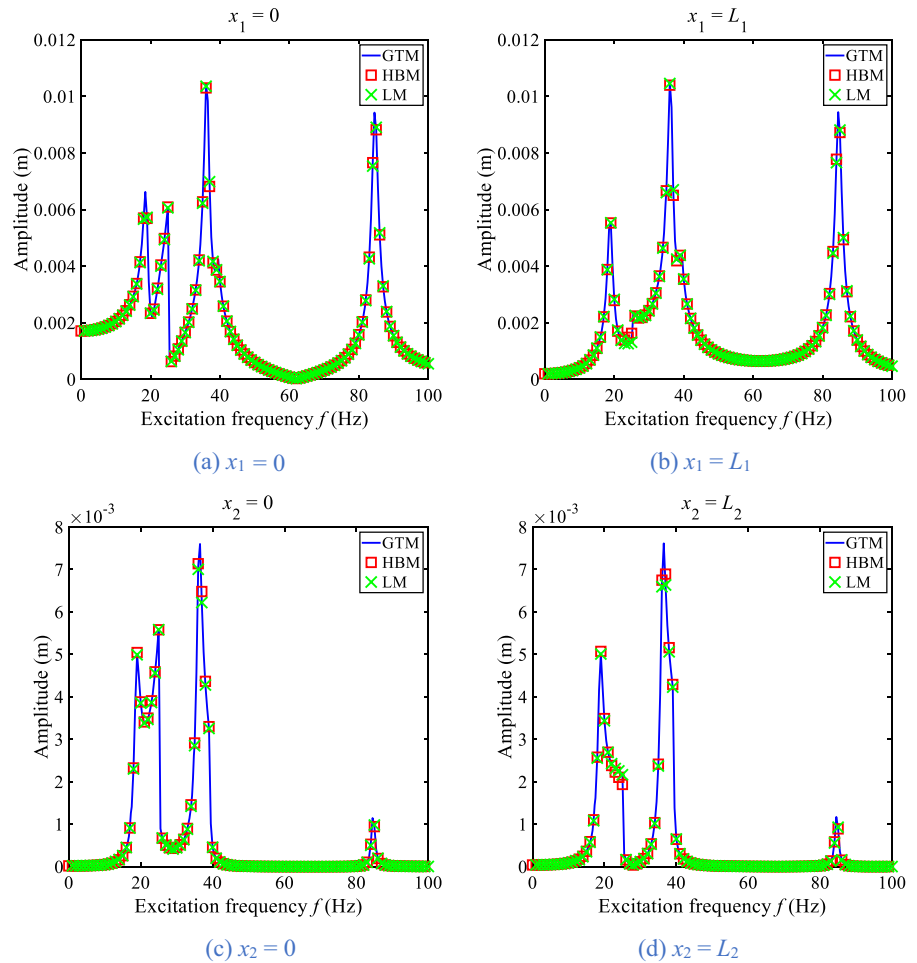




**Fig. 3** Amplitude-frequency curves of the double-beam connected through a mass-spring system that is nonlinear obtained through different methods



frequency curves of the double-beam system connected through a mass-spring system that is nonlinear under different methods. According to Fig. 3, amplitude-frequency curves obtained by the above three methods accurately match each other. Furthermore, in order to increase the credibility of the GTM results, Fig. 4 presents the stable time diagrams at both ends of the double-beam system predicted by the GTM, HBM, and LM, where the external excitation frequency is selected as 30 Hz. From Fig. 4, stable time diagrams predicted by the GTM, HBM, and LM match each other well. In summary, the phenomenon in Figs. 3 and 4 verifies the correctness of the GTM in predicting the dynamic behavior of the double-beam connected through a mass-spring system that is nonlinear.

Secondly, the stability of the GTM in predicting amplitude-frequency curves of the double-beam connected through a mass-spring system that is nonlinear

is studied. Amplitude-frequency curves with different truncation number are graphed in Fig. 5. According to Fig. 5, amplitude-frequency curves stay stable as the truncation number is 4-term, 6-term, and 8-term. In the following study, we choose 6-term as the truncation number of GTM.

### 3.2 Amplitude-frequency curves influenced by the mass-spring system that is nonlinear

This section investigates the influence of mass-spring system that is nonlinear on amplitude-frequency curves. Firstly, investigate the influence of nonlinear stiffness ( $kn_E = kn_{E1} = kn_{E2}$ ) on amplitude-frequency curves.  $kn_E$  is selected as  $0 \text{ N/m}^3$ ,  $10^9 \text{ N/m}^3$ ,  $2 \times 10^9 \text{ N/m}^3$ ,  $3 \times 10^9 \text{ N/m}^3$ . Amplitude-frequency curves of the double-beam connected through a mass-spring system that is nonlinear under different  $kn_E$  are

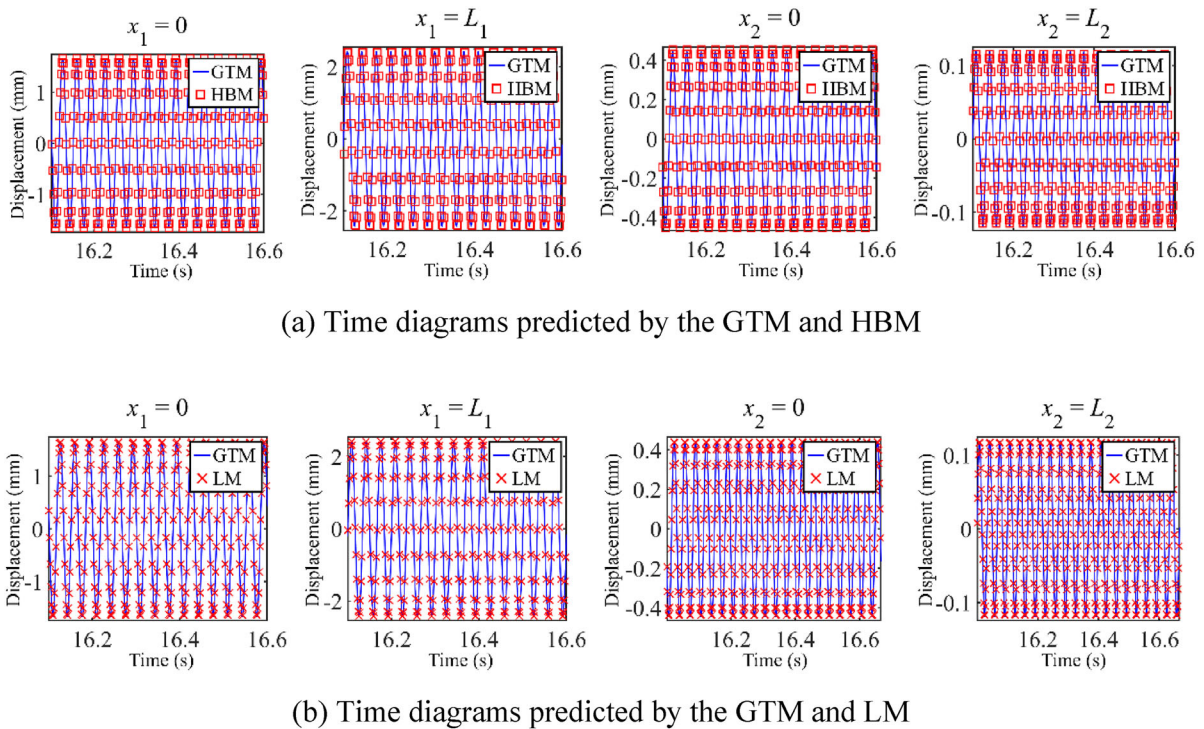


**Fig. 4** Time diagrams at both ends of the double-beam connected through a mass-spring system that is nonlinear predicted by different methods (30 Hz)

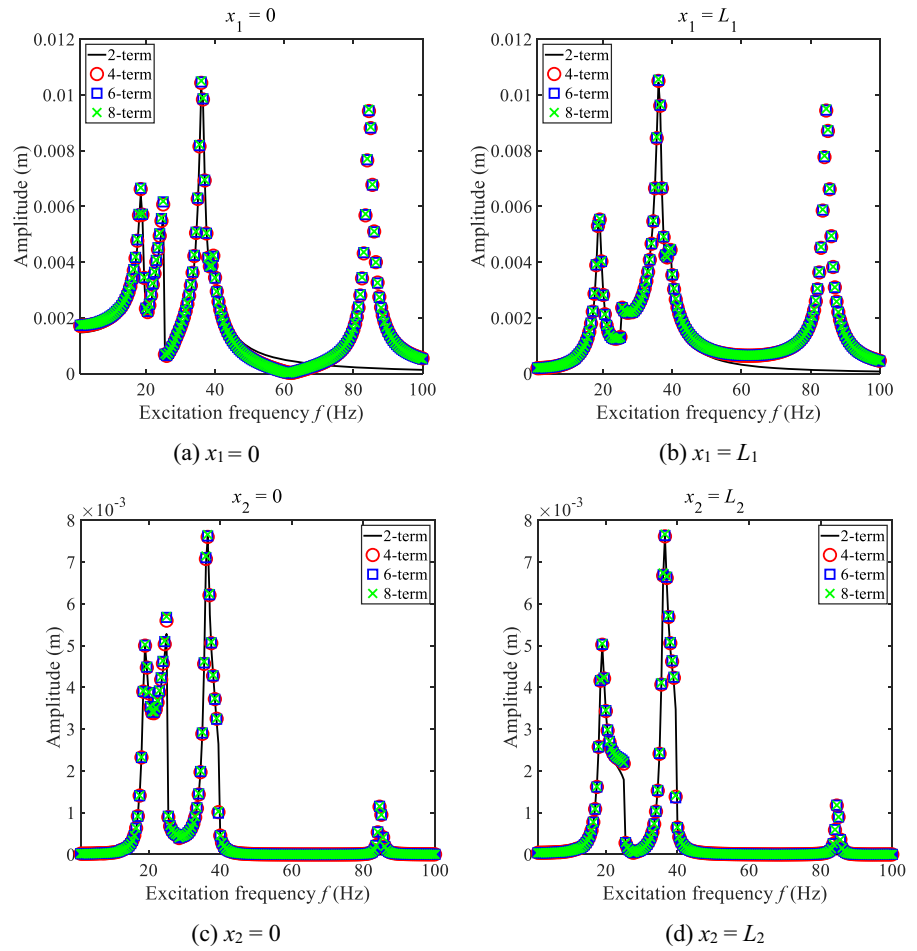
shown in Fig. 6. From Fig. 6, three primary resonance regions appear in amplitude-frequency curves under  $kn_E = 0 \text{ N/m}^3$  while there are four primary resonance regions in amplitude-frequency curves under  $10^9 \text{ N/m}^3$ ,  $2 \times 10^9 \text{ N/m}^3$ , and  $3 \times 10^9 \text{ N/m}^3$ . Such a phenomenon suggests that an additional resonance region is introduced in amplitude-frequency curves due to the mass-spring system that is nonlinear. Additionally, amplitude-frequency curves are no longer symmetric and peaks jump in the 2nd and 3rd resonance regions. The increase of  $kn_E$  suppresses the vibration at the 3rd primary resonance region. In the 2nd primary resonance region, the complex dynamic behavior appears with the increase of  $kn_E$ . The reason for such a phenomenon is that the nonlinear restoring force of Beam I and Beam II is proportional to the nonlinear stiffness of the mass-spring system which is nonlinear according to the definition of the nonlinear restoring force. When the other parameters of the mass-spring system that is nonlinear are determined, the nonlinear restoring force increases with the increases of the nonlinear mass-spring system's nonlinear stiffness. Furthermore, phase diagrams are graphed in Fig. 6 to

further study the complex dynamic behavior. According to subplots in Fig. 6, a closed curve is formed by Poincaré points, illustrating the state of complex dynamic behavior in Fig. 6 is quasi-periodic.

To explain the amplitude jumping phenomenon appears in the 2nd and 3rd resonance regions in Fig. 6, the max amplitude of the nonlinear restoring force acts on Beam I and Beam II with the variation of the excitation frequency is plotted in Fig. 7. From Fig. 7, the nonlinear restoring force jumps at the 2nd and 3rd resonance regions while the nonlinear restoring force keeps continuous at the 1st and 4th resonance regions. Due to the jump of the nonlinear restoring force, the amplitude jump phenomenon appears in amplitude-frequency response curves of the double-beam connected through a mass-spring system that is nonlinear, where the jumping frequency of the amplitude-frequency curves is the same as the jumping frequency in Fig. 7.

Secondly, the influence of viscous damping ( $C_{E1} = C_{E2}$ ) on amplitude-frequency curves is studied, where  $C_E$  is selected as 5 Ns/m, 10 Ns/m, 20 Ns/m, and 40 Ns/m.  $kn_E$  is selected as  $3 \times 10^9 \text{ N/m}^3$  and

**Fig. 5** Amplitude-frequency curves of the double-beam connected through a mass-spring system that is nonlinear with different truncation number



other parameters of the mass-spring system that is nonlinear are the same as those in Sect. 3.1. Amplitude-frequency curves of the double-beam connected through a mass-spring system that is nonlinear under different  $C_E$  are graphed in Fig. 8. According to Fig. 8, peaks jump at the 2nd and 3rd resonance regions. The increase of  $C_E$  is good for the vibration of the double-beam system. In the 2nd primary resonance region, the complex dynamic behavior appears when  $C_E = 5$  Ns/m. The complex dynamic behavior and amplitude-jumping phenomenon disappear with the increase of  $C_E$ . The reason for such a phenomenon is that the nonlinear restoring force acts on Beam I and Beam II is positively correlated with the relative displacement at the coupling position. The increase of  $C_E$  suppresses the peak amplitude at each primary resonance region of the double-beam system, suggesting the nonlinear restoring force at primary resonance regions decreases with the increase of  $C_E$ . The same as

the analysis in Fig. 6, the vibration state of the complex dynamic behavior in Fig. 8 is quasi-periodic.

Thirdly, the influence of concentrated mass ( $m_E$ ) on amplitude-frequency curves is studied, where  $m_E$  is selected as 0.005, 0.01, 0.02, and 0.03 kg.  $kn_E$  is selected as  $2 \times 10^9$  N/m<sup>3</sup> and other parameters of the mass-spring system that is nonlinear are shown in Table 2. Amplitude-frequency curves of the double-beam connected through a mass-spring system that is nonlinear under different  $m_E$  are graphed in Fig. 9. From Fig. 9, an amplitude-jumping phenomenon occurs at the 2nd and 3rd resonance regions. The change of  $m_E$  slightly influences the resonance regions' peaks. In the 4th primary resonance region, the complex dynamic behavior occurs when  $m_E = 0.03$  kg. The reason for the corresponding phenomenon is that the influence of  $m_E$  on the peak amplitude of the primary resonance regions is non-monotonic, suggesting the nonlinear restoring force

**Fig. 6** Amplitude-frequency curves of the double-beam connected through a mass-spring system that is nonlinear under different  $kn_E$

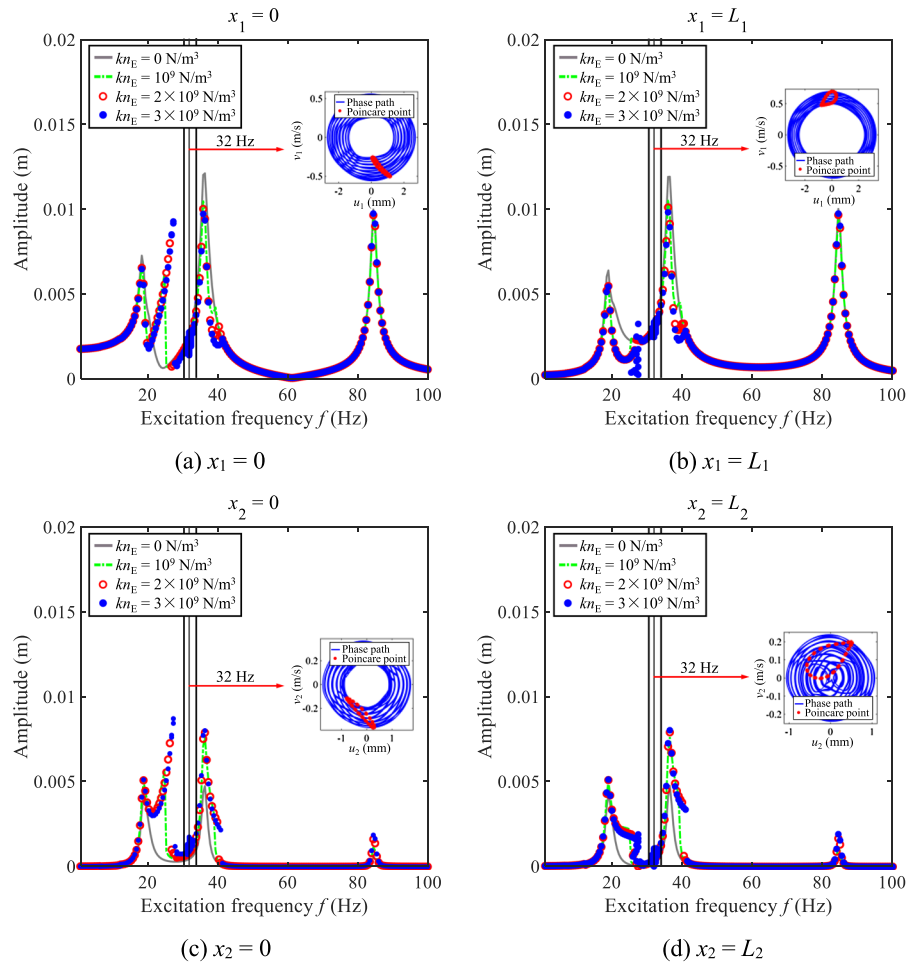
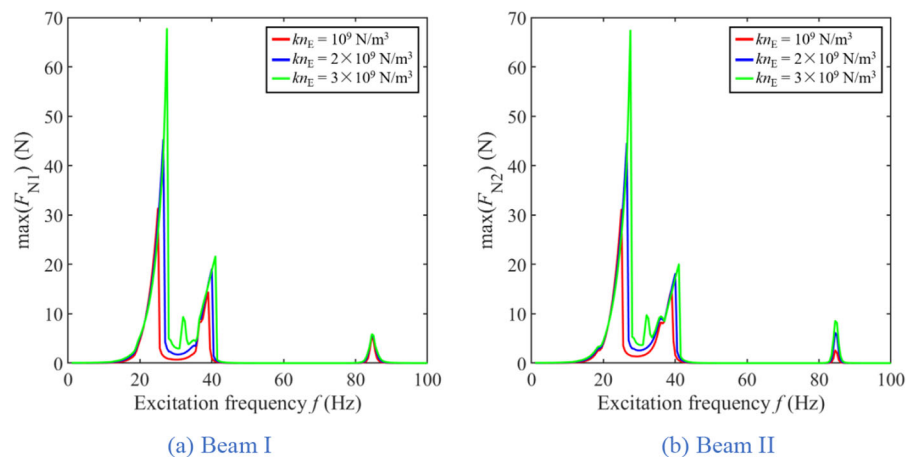


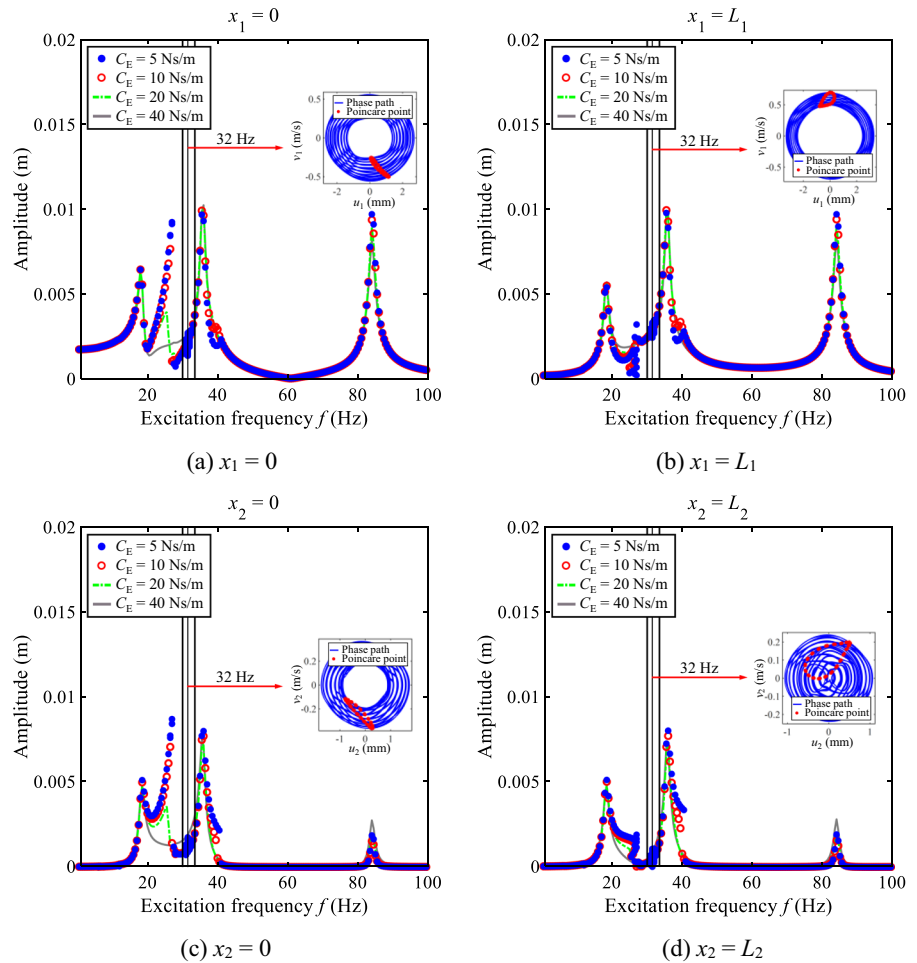
**Fig. 7** The max amplitude of the nonlinear restoring force acts on Beam I and Beam II with the variation of the excitation frequency



acts on Beam I and Beam II change nonmonotonic with the increase of  $m_E$ . Phase diagrams of the corresponding dynamic behavior are graphed.

According to each subplot in Fig. 9, a closed curve is formed by Poincaré points, suggesting the state of complex dynamic behavior in Fig. 8 is quasi-periodic.

**Fig. 8** Amplitude-frequency curves of the double-beam connected through a mass-spring system that is nonlinear under different  $C_E$



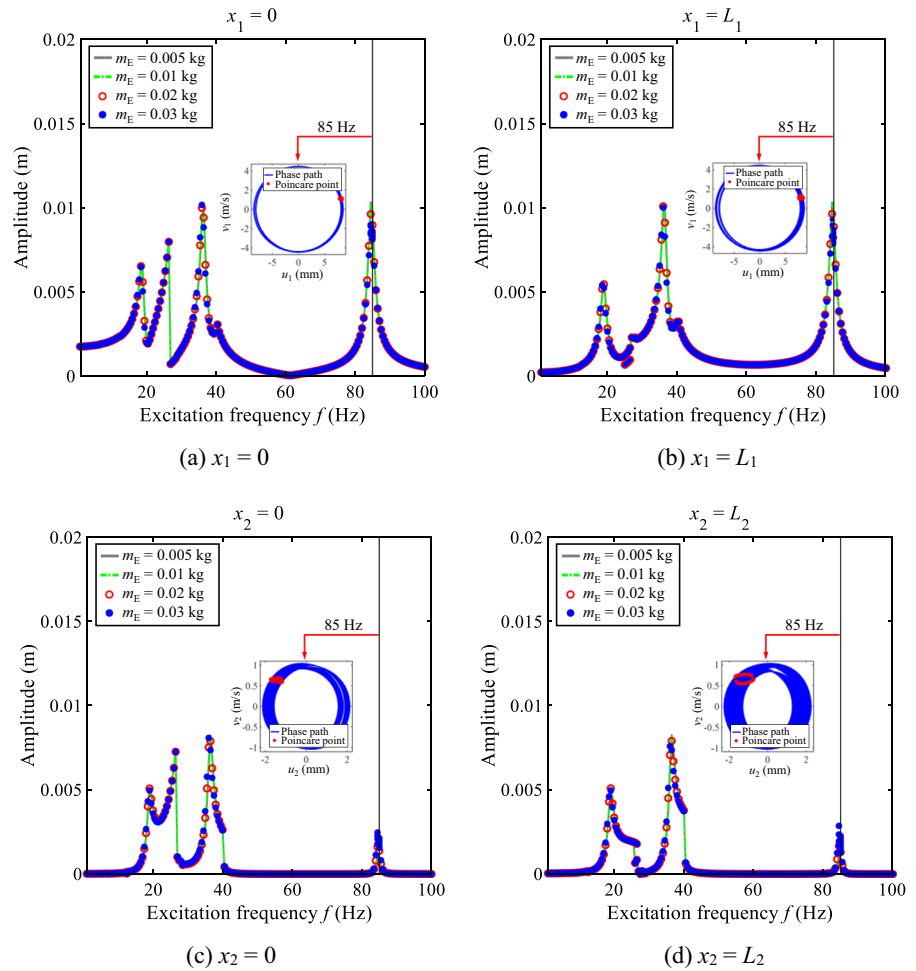
Fourthly, the influence of coupling position ( $x_{E1} = x_{E2} = x_E$ ) on amplitude-frequency curves is studied, where  $x_E$  is selected as 0.2, 0.4, 0.6, and 0.8 m.  $kn_E$  is selected as  $1.5 \times 10^9 \text{ N/m}^3$  and other parameters of the mass-spring system that is nonlinear are shown in Table 2. Amplitude-frequency curves of the double-beam connected through a mass-spring system that is nonlinear under different  $x_E$  are graphed in Fig. 10. According to Fig. 10, an amplitude-jumping phenomenon occurs at the 2nd and 3rd primary resonance regions. A suitable parameter of  $x_E$  can beneficially suppress the vibration at the boundary of the double-beam system. Furthermore, in the 3rd primary resonance region, the complex dynamic behavior occurs when  $x_E = 0.4 \text{ m}$ . The reason for the corresponding phenomenon is that the influence of  $x_E$  on the peak amplitude of the primary resonance regions is non-monotonic, suggesting the nonlinear restoring force

acts on Beam I and Beam II change nonmonotonic with the increase of  $x_E$ . Phase diagrams of the corresponding dynamic behavior are graphed. It can be seen from each subplot in Fig. 10 that a closed curve is formed by Poincaré points. The state of complex dynamic behavior in Fig. 10 is quasi-periodic.

To further study the double-beam system influenced by the mass-spring system that is nonlinear, the kinetic energy of the double-beam system under the complex dynamic behavior in Figs. 6, 8, 9, and 10 are graphed in Fig. 11. Combinations of the mass-spring system that is nonlinear and excitation frequency are shown in Table 3.

From Fig. 11, the kinetic energy of beams is higher than the mass-spring system which is nonlinear. In the time interval  $T_s$ , the kinetic energy of Beam I targeted transfers to Beam II. For other time intervals, the

**Fig. 9** Amplitude-frequency curves of the double-beam connected through a mass-spring system that is nonlinear under different  $m_E$



kinetic energy of Beam II targeted transfers to Beam I. It should be noticed that the vibration state of the complex dynamic behavior in Figs. 6, 8, 9, and 10 is quasi-periodic, indicating that the quasi-periodic vibration state of the double-beam connected through a mass-spring system that is nonlinear can be regarded as a sign of the occurrence of the targeted energy transfer.

### 3.3 Single-frequency responses influenced by the mass-spring system that is nonlinear

This section investigates the influence of the mass-spring system that is nonlinear on single-frequency responses. For this section, the excitation frequency is selected as 38 Hz and the parameters of the double-beam system are shown in Table 1. In plotting dynamic responses of the double-beam system with

the variation of the mass-spring system's parameters, the maximum value of the time-domain responses of the double-beam system under the single excitation frequency is selected as the  $y$  coordinate while parameters of the mass-spring system that is nonlinear are selected as the  $x$  coordinate.

Firstly, study the influence of nonlinear stiffness ( $kn_E = kn_{E1} = kn_{E2}$ ) on single-frequency responses. Figure 12 depicts single-frequency responses of the double-beam with the change of  $kn_E$ . According to Fig. 12, as  $kn_E$  ranges from  $10^{8.3}$  to  $10^{9.7}$  N/m<sup>3</sup>, the increase of  $kn_E$  is good at vibration suppression at the boundary of Beam I. Furthermore, there are two unstable regions [ $10^{9.7}$  N/m<sup>3</sup>,  $10^{11.1}$  N/m<sup>3</sup>], [ $10^{11.8}$  N/m<sup>3</sup>,  $10^{12}$  N/m<sup>3</sup>] in single-frequency responses.  $10^{9.7}$  N/m<sup>3</sup>,  $10^{11.1}$  N/m<sup>3</sup>, and  $10^{11.8}$  N/m<sup>3</sup> are defined as the converted values of  $kn_E$ . Changing  $kn_E$  around its converted values significantly changes the

**Fig. 10** Amplitude-frequency curves of the double-beam connected through a mass-spring system that is nonlinear under different  $x_E$

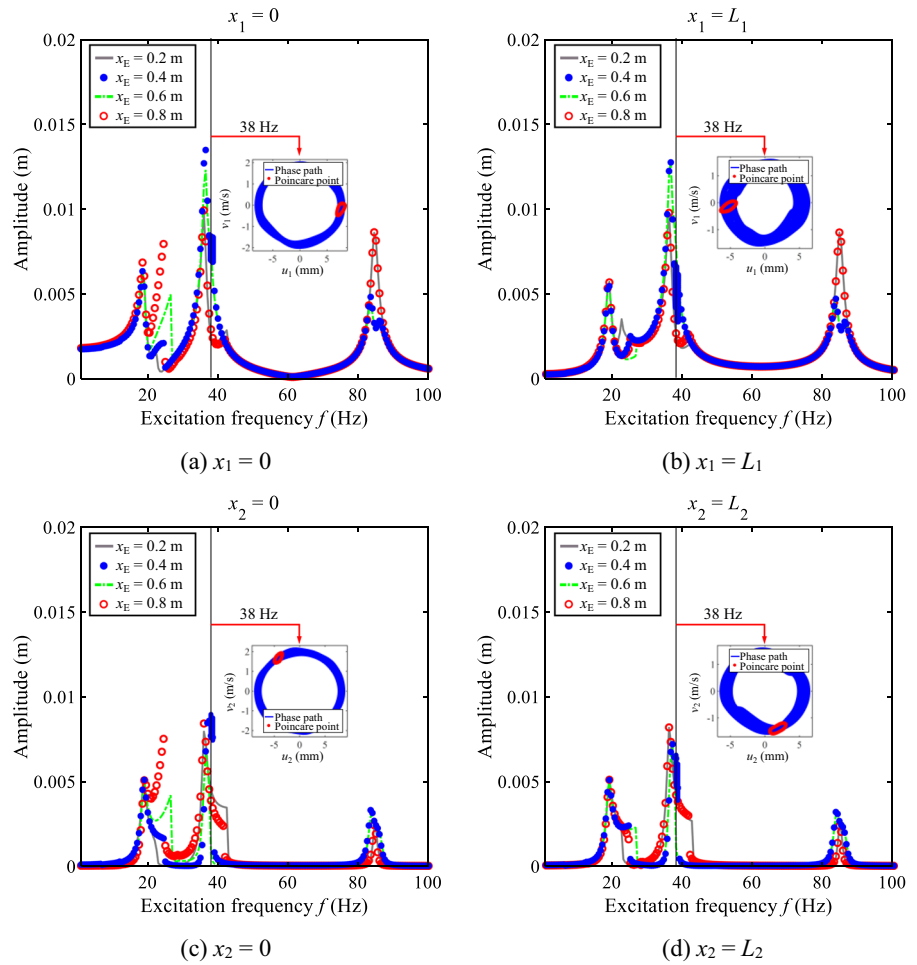
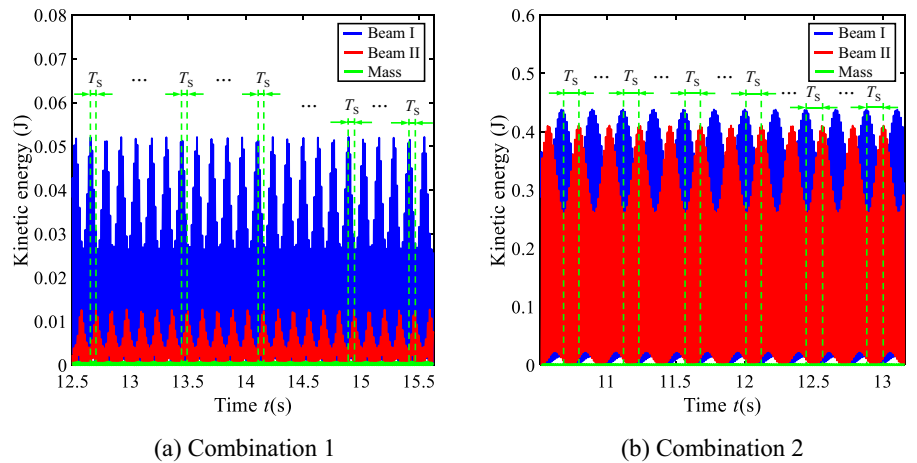


**Fig. 11** Kinetic energy of the double-beam connected through a mass-spring system that is nonlinear



vibration state of the vibration system. With the continuous increase of  $kn_E$ , the variation of the complex dynamic behavior in the single-frequency

responses of the double-beam system with the change of  $kn_E$  is nonmonotonic. The reason for such a phenomenon is that resonance regions of the

**Table 3** Combinations of the mass-spring system that is nonlinear and excitation frequency

Combination 1	Combination 2
$m_E = 0.02$ kg	$m_E = 0.02$ kg
$x_{E1} = x_{E2} = 0.7$ m	$x_{E1} = x_{E2} = 0.4$ m
$C_{E1} = C_{E2} = 5$ Ns/m	$C_{E1} = C_{E2} = 5$ Ns/m
$k_{E1} = k_{E2} = 10^3$ N/m	$k_{E1} = k_{E2} = 10^3$ N/m
$kn_{E1} = kn_{E2} = 3 \times 10^9$ N/m <sup>3</sup>	$kn_{E1} = kn_{E2} = 1.5 \times 10^9$ N/m <sup>3</sup>
$f = 32$ Hz	$f = 38$ Hz

amplitude-frequency curve shift to higher frequency regions with the increase of  $kn_E$ . In the single-frequency responses, the excitation frequency is determined as 38 Hz, which is near the 2nd and 3rd primary resonance region of the amplitude-frequency response curves. In the process of increasing  $kn_E$ , the

2nd and 3rd primary resonance regions of the amplitude-frequency response curves cross 38 Hz. In the above process, the nonlinear restoring force acting on Beam I and Beam II changes nonmonotonically, causing the nonmonotonic change of the complex dynamic behavior. Then, phase diagrams of the unstable regions are graphed. In each subplot in Fig. 12, a closed curve is formed by Poincaré points, which can be concluded that the vibration state of the unstable regions is quasi-periodic.

Secondly, study the influence of viscous damping ( $C_E = C_{E1} = C_{E2}$ ) on single-frequency responses.  $kn_E$  is selected as  $10^{10}$  N/m<sup>3</sup> and other parameters of the mass-spring system that is nonlinear are the same as those in Sect. 3.1. Single-frequency responses of the double-beam with the change of  $C_E$  are graphed in Fig. 13. According to Fig. 13, when  $C_E$  in the region [13.5 Ns/m to 52 Ns/m], the increase of  $C_E$  is good at

**Fig. 12** Single-frequency responses of the double-beam connected through a mass-spring system that is nonlinear with the change of  $kn_E$

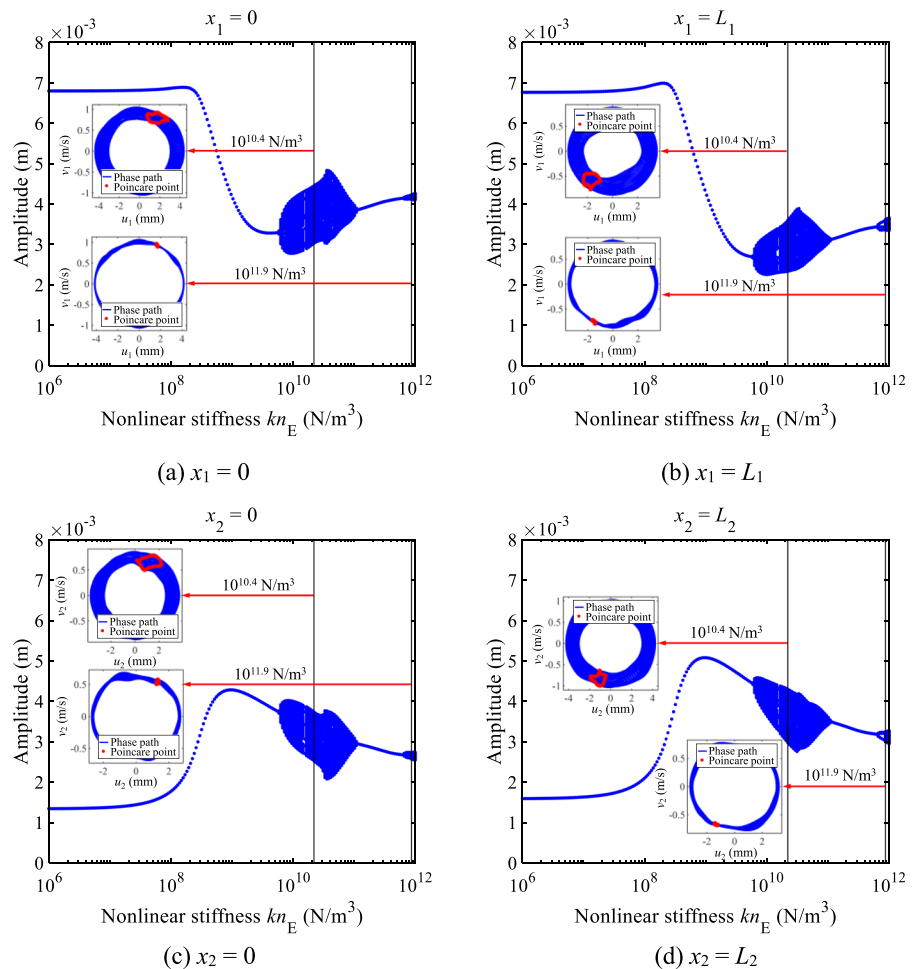
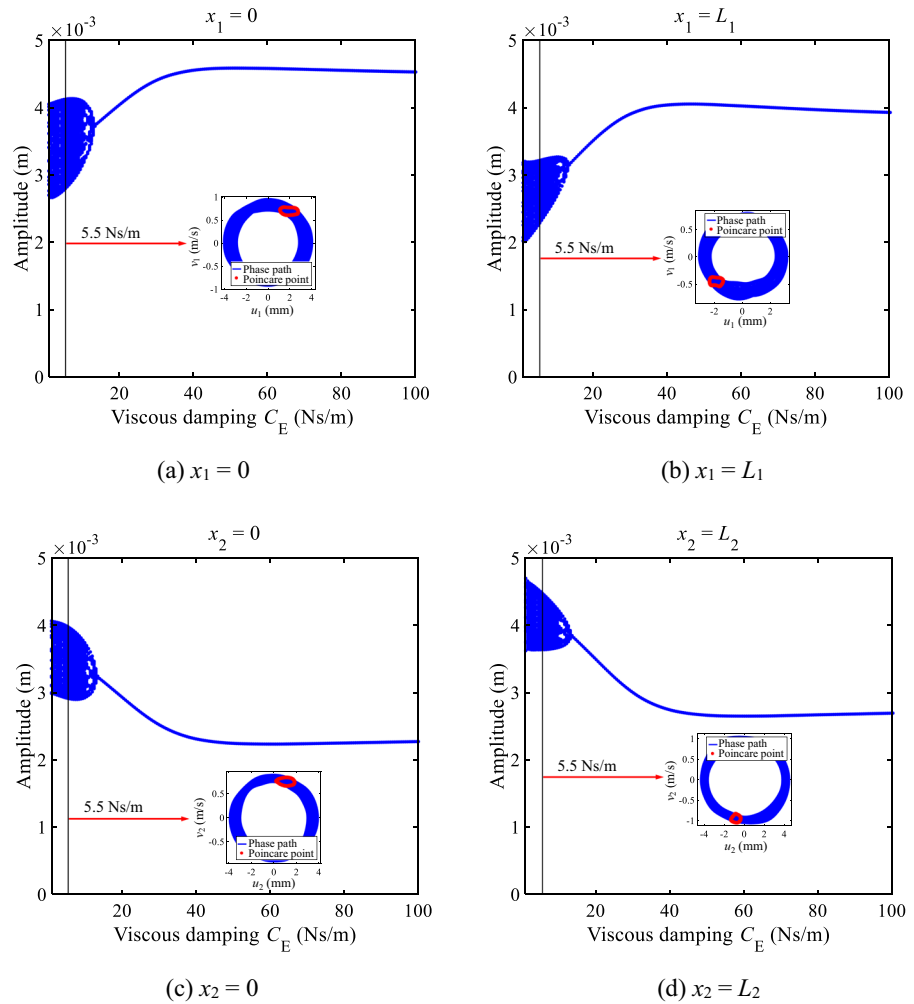




**Fig. 13** Single-frequency responses of the double-beam connected through a mass-spring system that is nonlinear with the change of  $C_E$

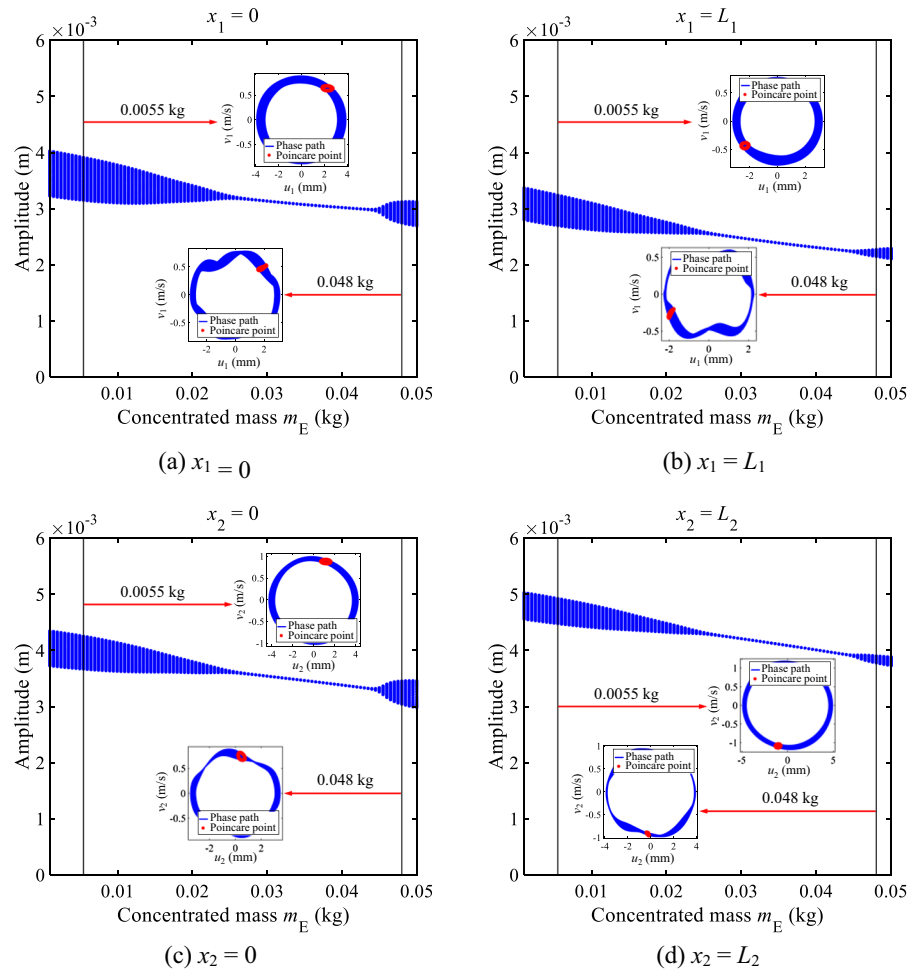


vibration suppression at the boundary of Beam II. There is an unstable region [1 Ns/m, 13.5 Ns/m] in single-frequency responses. 13.5 Ns/m is defined as the converted value of  $C_E$ . The vibration state of the double-beam changes greatly when  $C_E$  changes around its converted value. After  $C_E$  exceeds its converted value, the unstable region of the double-beam system vanishes. Furthermore, with the continuous increase of  $C_E$ , the variation of the complex dynamic behavior in the single-frequency responses of the double-beam system with the change of  $C_E$  is monotonic. The reason for such a phenomenon is that resonance regions of the amplitude-frequency curve shift to lower frequency regions with the increase of  $C_E$  under certain  $kn_E$ . In the process of increasing  $C_E$ , the 3rd primary resonance region of the amplitude-frequency response curves monotonically crosses

38 Hz. In the above process, the nonlinear restoring force acting on Beam I and Beam II changes monotonically, causing the monotonic change of the complex dynamic behavior. Phase diagrams of the unstable region are graphed. It can be seen from Fig. 13 that a closed curve is formed by Poincaré points in each subplot while phase diagrams stay stable. The above phenomenon suggests that the vibration state of the unstable region is quasi-periodic.

Thirdly, study the influence of concentrated mass ( $m_E$ ) on single-frequency response. Single-frequency responses with the change of  $m_E$  are graphed in Fig. 14.  $kn_E$  is selected as  $6 \times 10^9$  N/m<sup>3</sup> and other parameters of the mass-spring system that is nonlinear are the same as those employed in Sect. 3.1. From Fig. 14, when  $m_E$  is in the region [0.0265 kg, 0.044 kg], the increase of  $m_E$  is good at the vibration

**Fig. 14** Single-frequency responses of the double-beam connected through a mass-spring system that is nonlinear with the change of  $m_E$



suppression at the boundary of the double-beam. There are two unstable regions [0.001 kg, 0.0265 kg], [0.044 kg, 0.05 kg] in single-frequency responses, 0.0265 kg and 0.044 kg are defined as the converted values of  $m_E$ . Changing  $m_E$  around its converted values significantly changes the state of the vibration system. The variation of the complex dynamic behavior in the single-frequency responses of the double-beam system with the increase of  $m_E$  is nonmonotonic. The reason for such a phenomenon is that the position of resonance regions of the amplitude-frequency curve is influenced by  $m_E$ , where the influence of  $m_E$  on the position of the primary resonance regions is nonmonotonic. In the increase process of increasing  $m_E$ , the 3rd primary resonance region of the amplitude-frequency response curve crosses 38 Hz multiple times. In the above process, the nonlinear restoring force acting on Beam I and Beam

II changes nonmonotonically, causing the nonmonotonic change of the complex dynamic behavior. To deeply study the unstable regions' dynamic responses, phase diagrams of the corresponding regions are graphed. The same as the analysis in Figs. 12 and 13, the state of unstable regions in Fig. 14 is quasi-periodic.

Fourthly, investigate the influence of coupling position ( $x_E = x_{E1} = x_{E2}$ ) on single-frequency responses. Single-frequency responses with the change of  $x_E$  are graphed in Fig. 15.  $kn_E$  is selected as  $2 \times 10^9$  N/m<sup>3</sup> and other parameters of the mass-spring system that is nonlinear are the same as those employed in Sect. 3.1. According to Fig. 15, the increase of  $x_E$  is good at the vibration suppression at the boundary of the double-beam when  $x_E$  changes from 0.6 to 0.9 m. Additionally, when  $x_E$  ranges from 0.43 to 0.6 m, the vibration at the boundary of Beam II

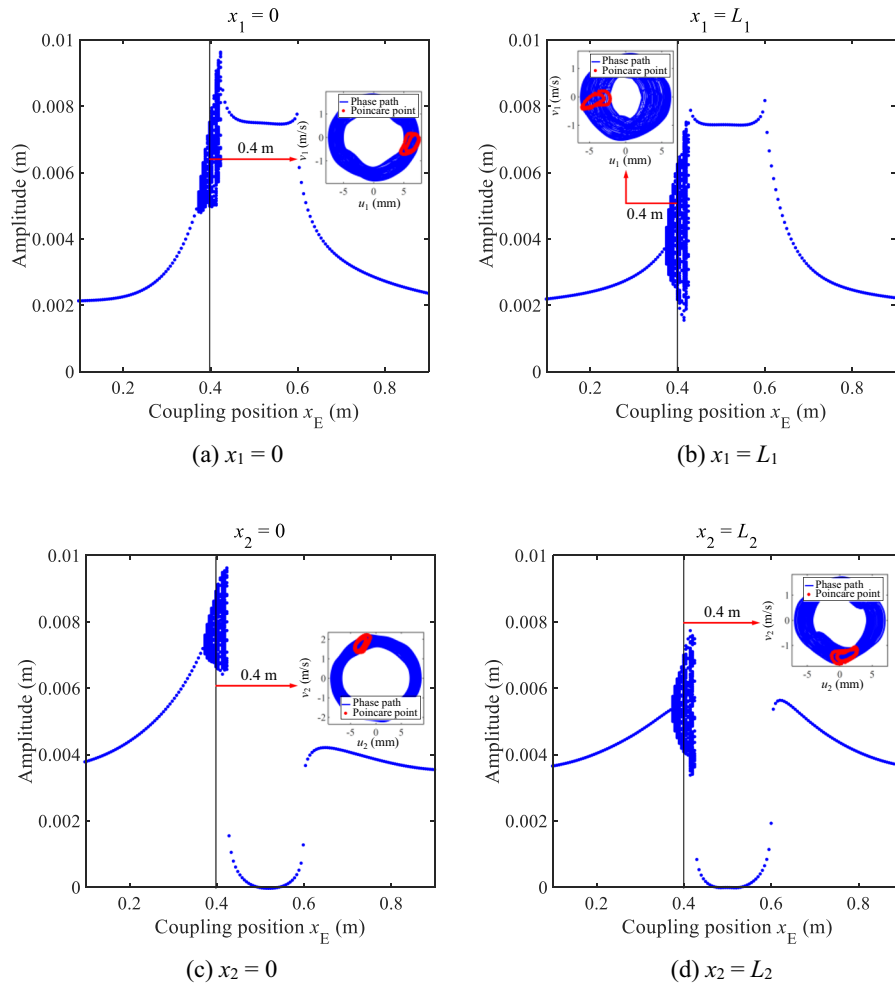


**Fig. 15** Single-frequency responses of the double-beam structure connected through a mass-spring system that is nonlinear with the change of  $x_E$

stays at a low level. An unstable region [0.37 m, 0.425 m] appears in single-frequency responses. 0.37 m and 0.425 m are defined as the converted values of  $x_E$ . The vibration state of the double-beam changes obviously when  $x_E$  varies around its converted values. The variation of the complex dynamic behavior in the single-frequency responses of the double-beam system with the increase of  $x_E$  is nonmonotonic. The reason for such a phenomenon is that the position of resonance regions of the amplitude-frequency curve is influenced by  $x_E$ , where the influence of  $x_E$  on the position of the primary resonance regions is nonmonotonic. In the process of increasing  $x_E$ , the 3rd primary resonance region of the amplitude-frequency response curve crosses 38 Hz multiple times. In the above process, the nonlinear

restoring force acting on Beam I and Beam II changes nonmonotonically, causing the nonmonotonic change of the complex dynamic behavior. Furthermore, phase diagrams of the unstable regions are graphed. The same as the analysis in Figs. 12 and 13, the unstable region’s vibration state in Fig. 15 is quasi-periodic.

To deeply study single-frequency responses influenced by the mass-spring system that is nonlinear, the kinetic energy of the double-beam under the complex dynamic behavior in Figs. 12, 13, 14, and 15 are graphed in Fig. 16. Combinations of the mass-spring system that is nonlinear are shown in Table 4.

From Fig. 16, the kinetic energy of the concentrated mass is lower than that of beams. Due to the existence of the mass-spring system that is nonlinear,

**Fig. 16** Kinetic energy of the double-beam connected through a mass-spring system that is nonlinear

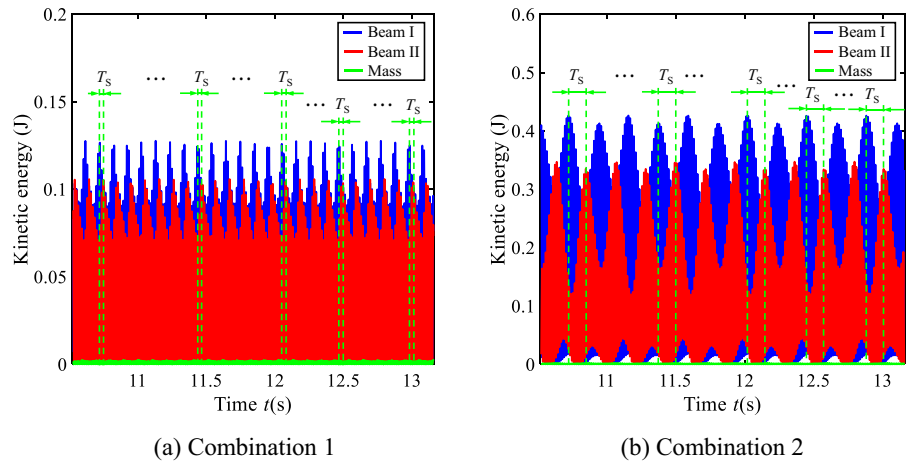


**Table 4** Combinations of the mass-spring system that is nonlinear

Combination 1	Combination 2
$m_E = 0.02 \text{ kg}$	$m_E = 0.02 \text{ kg}$
$x_{E1} = x_{E2} = 0.7 \text{ m}$	$x_{E1} = x_{E2} = 0.4 \text{ m}$
$C_{E1} = C_{E2} = 5 \text{ Ns/m}$	$C_{E1} = C_{E2} = 5 \text{ Ns/m}$
$k_{E1} = k_{E2} = 10^3 \text{ N/m}$	$k_{E1} = k_{E2} = 10^3 \text{ N/m}$
$kn_{E1} = kn_{E2} = 10^{10.4} \text{ N/m}^3$	$kn_{E1} = kn_{E2} = 2 \times 10^9 \text{ N/m}^3$

the kinetic energy of Beam I targeted transfers to Beam II under the time interval  $T_s$ . For other time intervals, the kinetic energy of Beam II targeted transfers to Beam I. Furthermore, according to the analysis in Figs. 12, 13, 14, and 15, the vibration state of the complex dynamic behavior is quasi-periodic. The quasi-periodic vibration state corresponds to the targeted energy transfer phenomenon between beams, suggesting the quasi-periodic vibration state of the double-beam connected through a mass-spring system that is nonlinear can be regarded as a sign of the occurrence of the targeted energy transfer.

### 4 Conclusion

In this study, the nonlinear dynamic behavior of an elastically restrained double-beam connected through a mass-spring system that is nonlinear is investigated. Using the variational method and the generalized Hamiltonian method build the corresponding system’s governing functions. Then, applying the Galerkin

truncation method predicts the dynamic behavior of the double-beam connected through a mass-spring system that is nonlinear, where the harmonic balanced method and Lagrange method are employed to verify the correctness of the results obtained by the Galerkin truncation method. On this basis, the influence of a mass-spring system that is nonlinear on amplitude-frequency curves and single-frequency responses of an elastically restrained double-beam is investigated. For the structural parameters and boundary conditions of the double-beam system employed in this study, some conclusions are made.

- (1) The GTM has good stability and correctness in predicting dynamic responses of the double-beam connected through a mass-spring system that is nonlinear. For this study, a 4-term truncation number can keep the stability of the GTM.
- (2) Amplitude-frequency and single-frequency responses of the double-beam are both significantly influenced by changing parameters of the mass-spring system that is nonlinear. The amplitude jumping phenomenon and complex dynamic behavior of the double-beam occurs under certain parameters of the mass-spring system that is nonlinear. Around converted values of the mass-spring system that is nonlinear, the dynamic behavior of the double-beam can be easily changed.
- (3) The complex dynamic behavior of the double-beam system changes characteristics of the double-beam system’s kinetic energy transfer, where the vibration state of the double-beam

system’s complex dynamic behavior is quasi-periodic. A quasi-periodic vibration state can be regarded as a sign of the occurrence of the targeted energy transfer of the double-beam connected through a mass-spring system that is nonlinear.

- (4) On the whole, changing parameters of the mass-spring system that is nonlinear can significantly influence the dynamic behavior of the double-beam while suitable parameters of the mass-spring system that is nonlinear are good at vibration suppression at the boundary of the double-beam.

**Acknowledgements** This work is supported by the National Natural Science Foundation of China (Grant No. 11972125 and 12102101).

**Data availability** The datasets generated during and/or analyzed during the current study are available from the corresponding author upon reasonable request.

**Declarations**

**Conflict of interest** The authors declare no conflict of interest in preparing this article.

**Human or animal rights** No human or animal subjects were used in this work.

**Appendix A**

$$V_{BeamI} = \int_0^{L_1} \frac{1}{2} E_1 I_1 \left( \frac{\partial^2 u_1}{\partial x_1^2} \right)^2 dx_1 \tag{A1}$$

$$V_{BeamII} = \int_0^{L_2} \frac{1}{2} E_2 I_2 \left( \frac{\partial^2 u_2}{\partial x_2^2} \right)^2 dx_2 \tag{A2}$$

$$V_{BoundaryI} = \frac{1}{2} k_{L1} [u_1(0, t)]^2 + \frac{1}{2} k_{R1} [u_1(L_1, t)]^2 + \frac{1}{2} K_{L1} \left[ \frac{\partial u_1(0, t)}{\partial x_1} \right]^2 + \frac{1}{2} K_{R1} \left[ \frac{\partial u_1(L_1, t)}{\partial x_1} \right]^2 \tag{A3}$$

$$V_{BoundaryII} = \frac{1}{2} k_{L2} [u_2(0, t)]^2 + \frac{1}{2} k_{R2} [u_2(L_2, t)]^2 + \frac{1}{2} K_{L2} \left[ \frac{\partial u_2(0, t)}{\partial x_2} \right]^2 + \frac{1}{2} K_{R2} \left[ \frac{\partial u_2(L_2, t)}{\partial x_2} \right]^2 \tag{A4}$$

$$V_E = \frac{1}{2} k_{E1} [u_E - u_1(x_{E1}, t)]^2 + \frac{1}{2} k_{E2} [u_E - u_2(x_{E2}, t)]^2 + \frac{1}{4} kn_{E1} [u_E - u_1(x_{E1}, t)]^4 + \frac{1}{4} kn_{E2} [u_E - u_2(x_{E2}, t)]^4 \tag{A5}$$

$$T_I = \int_0^{L_1} \frac{1}{2} \rho_1 S_1 \left( \frac{\partial u_1}{\partial t} \right)^2 dt \tag{A6}$$

$$T_{II} = \int_0^{L_2} \frac{1}{2} \rho_2 S_2 \left( \frac{\partial^2 u_2}{\partial t^2} \right)^2 dt \tag{A7}$$

$$T_E = \frac{1}{2} m_E \left( \frac{du_E}{dt} \right)^2 \tag{A8}$$

$$\delta W_{C1} = - \int_0^{L_1} C_{B1} \frac{\partial u_1}{\partial t} \delta u_1 dx_1 \tag{A9}$$

$$\delta W_{C2} = - \int_0^{L_2} C_{B2} \frac{\partial u_2}{\partial t} \delta u_2 dx_2 \tag{A10}$$

$$\delta W_{CE1} = -C_{E1} \left[ \frac{\partial u_E}{\partial t} - \frac{\partial u_1(x_{E1}, t)}{\partial t} \right] \delta [u_E - u_1(x_{E1}, t)] \tag{A11}$$

$$\delta W_{CE2} = -C_{E2} \left[ \frac{\partial u_E}{\partial t} - \frac{\partial u_2(x_{E2}, t)}{\partial t} \right] \delta [u_E - u_2(x_{E2}, t)] \tag{A12}$$

$$\delta W_{F1} = - \int_0^{L_1} \delta(x_1 - L_1) F_1 \sin(\omega t) \delta u_1 dx_1 \tag{A13}$$

## Appendix B

$$\int_{t_1}^{t_2} \delta V_{\text{BeamI}} dt = \int_{t_1}^{t_2} \int_0^{L_1} E_1 I_1 \frac{\partial^4 u_1}{\partial x_1^4} \delta u_1 dx_1 dt + \int_{t_1}^{t_2} \left[ E_1 I_1 \frac{\partial^2 u_1(L_1, t)}{\partial x_1^2} \delta \left( \frac{\partial u_1}{\partial x_1} \right) - E_1 I_1 \frac{\partial^3 u_1(L_1, t)}{\partial x_1^3} \delta u_1 - E_1 I_1 \frac{\partial^2 u_1(0, t)}{\partial x_1^2} \delta \left( \frac{\partial u_1}{\partial x_1} \right) + E_1 I_1 \frac{\partial^3 u_1(0, t)}{\partial x_1^3} \delta u_1 \right] dt \quad (\text{B1})$$

$$\int_{t_1}^{t_2} \delta V_{\text{BeamII}} dt = \int_{t_1}^{t_2} \int_0^{L_2} E_2 I_2 \frac{\partial^4 u_2}{\partial x_2^4} \delta u_2 dx_2 dt + \int_{t_1}^{t_2} \left[ E_2 I_2 \frac{\partial^2 u_2(L_2, t)}{\partial x_2^2} \delta \left( \frac{\partial u_2}{\partial x_2} \right) - E_2 I_2 \frac{\partial^3 u_2(L_2, t)}{\partial x_2^3} \delta u_2 - E_2 I_2 \frac{\partial^2 u_2(0, t)}{\partial x_2^2} \delta \left( \frac{\partial u_2}{\partial x_2} \right) + E_2 I_2 \frac{\partial^3 u_2(0, t)}{\partial x_2^3} \delta u_2 \right] dt \quad (\text{B2})$$

$$\int_{t_1}^{t_2} \delta V_{\text{BoundaryI}} dt = \int_{t_1}^{t_2} \left[ k_{L1} u_1(0, t) \delta u_1 + K_{L1} \frac{\partial u_1(0, t)}{\partial x_1} \delta \left( \frac{\partial u_1}{\partial x_1} \right) + k_{R1} u_1(L_1, t) \delta u_1 + K_{R1} \frac{\partial u_1(L_1, t)}{\partial x_1} \delta \left( \frac{\partial u_1}{\partial x_1} \right) \right] dt \quad (\text{B3})$$

$$\int_{t_1}^{t_2} \delta V_{\text{BoundaryII}} dt = \int_{t_1}^{t_2} \left[ k_{L2} u_2(0, t) \delta u_2 + K_{L2} \frac{\partial u_2(0, t)}{\partial x_2} \delta \left( \frac{\partial u_2}{\partial x_2} \right) + k_{R2} u_2(L_2, t) \delta u_2 + K_{R2} \frac{\partial u_2(L_2, t)}{\partial x_2} \delta \left( \frac{\partial u_2}{\partial x_2} \right) \right] dt \quad (\text{B4})$$

$$\int_{t_1}^{t_2} \delta V_E dt = \int_{t_1}^{t_2} \left\{ \begin{array}{l} k_{E1} [u_E - u_1(x_{E1}, t)] \delta [u_E - u_1(x_{E1}, t)] \\ + k_{E2} [u_E - u_2(x_{E2}, t)] \delta [u_E - u_2(x_{E2}, t)] \\ + k_{nE1} [u_E - u_1(x_{E1}, t)]^3 \delta [u_E - u_1(x_{E1}, t)] \\ + k_{nE2} [u_E - u_2(x_{E2}, t)]^3 \delta [u_E - u_2(x_{E2}, t)] \end{array} \right\} dt \quad (\text{B5})$$

$$\int_{t_1}^{t_2} \delta T_I dt = - \int_{t_1}^{t_2} \int_0^{L_1} \rho_1 S_1 \frac{\partial^2 u_1}{\partial t} \delta u_1 dx_1 dt \quad (\text{B6})$$

$$\int_{t_1}^{t_2} \delta T_{II} dt = - \int_{t_1}^{t_2} \int_0^{L_2} \rho_2 S_2 \frac{\partial^2 u_2}{\partial t} \delta u_2 dx_2 dt \quad (\text{B7})$$

$$\int_{t_1}^{t_2} \delta T_E dt = - \int_{t_1}^{t_2} m_E \frac{d^2 u_E}{dt^2} \delta u_E dt \quad (\text{B8})$$

$$\int_{t_1}^{t_2} \delta W_{C1} dt = - \int_{t_1}^{t_2} \int_0^{L_1} C_{B1} \frac{\partial u_1}{\partial t} \delta u_1 dx_1 dt \quad (\text{B9})$$

$$\int_{t_1}^{t_2} \delta W_{C2} dt = - \int_{t_1}^{t_2} \int_0^{L_2} C_{B2} \frac{\partial u_2}{\partial t} \delta u_2 dx_2 dt \quad (\text{B10})$$

$$\int_{t_1}^{t_2} \delta W_{CE1} dt = - \int_{t_1}^{t_2} C_{E1} \left[ \frac{du_E}{dt} - \frac{\partial u_1(x_{E1}, t)}{\partial t} \right] \delta [u_E - u_1(x_{E1}, t)] dt \quad (\text{B11})$$

$$\int_{t_1}^{t_2} \delta W_{CE2} dt = - \int_{t_1}^{t_2} C_{E2} \left[ \frac{du_E}{dt} - \frac{\partial u_2(x_{E2}, t)}{\partial t} \right] \delta [u_E - u_2(x_{E2}, t)] dt \quad (\text{B12})$$

$$\int_{t_1}^{t_2} \delta W_{F1} dt = - \int_{t_1}^{t_2} \int_0^{L_1} \delta(x_1 - L_1) F_1 \sin(\omega t) \delta u_1 dx_1 dt \quad (\text{B13})$$

## Appendix C

$$RI_{m1} = \int_0^{L_1} \rho_1 S_1 \left[ \sum_{i=1}^{N_1} \varphi_{1i}(x_1) \frac{d^2 q_{1i}(t)}{dt^2} \right] \psi_{1m_1}(x_1) dx_1 \quad (\text{C1})$$

$$RI_{m2} = \int_0^{L_1} C_{B1} \left[ \sum_{i=1}^{N_1} \varphi_{1i}(x_1) \frac{dq_{1i}(t)}{dt} \right] \psi_{1m_1}(x_1) dx_1 \quad (\text{C2})$$

$$RI_{m3} = \int_0^{L_1} E_1 I_1 \left[ \sum_{i=1}^{N_1} \frac{d^4 \varphi_{1i}(x)}{dx_1^4} q_{1i}(t) \right] \psi_{1m_1}(x_1) dx_1 \quad (\text{C3})$$

$$RI_{m4} = \psi_{1m_1}(x_{F1}) F_1 \sin(\omega t) \quad (\text{C4})$$

$$RI_{m5} = C_{E1} \left[ \sum_{i=1}^{N_1} \varphi_{1i}(x_{E1}) \frac{dq_{1i}(t)}{dt} - u_E(t) \right] \psi_{1m_1}(x_{E1}) \quad (\text{C5})$$

$$RI_{m6} = k_{E1} \left[ \sum_{i=1}^{N_1} \varphi_{1i}(x_{E1}) q_{1i}(t) - u_E(t) \right] \psi_{1m_1}(x_{E1}) \quad (\text{C6})$$

$$RI_{m_17} = kn_{E1} \left[ \sum_{i=1}^{N_1} \varphi_{1i}(x_{E1})q_{1i}(t) - u_E(t) \right]^3 \psi_{1m_1}(x_{E1}) \tag{C7}$$

$$RII_{m_21} = \int_0^{L_2} \rho_2 S_2 \left[ \sum_{i=1}^{N_2} \varphi_{2i}(x_2) \frac{d^2 q_{2i}(t)}{dt} \right] \psi_{2m_2}(x_2) dx_2 \tag{C8}$$

$$RII_{m_22} = \int_0^{L_2} C_{B2} \left[ \sum_{i=1}^{N_2} \varphi_{2i}(x_2) \frac{dq_{2i}(t)}{dt} \right] \psi_{2m_2}(x_2) dx_2 \tag{C9}$$

$$RII_{m_23} = \int_0^{L_2} E_2 I_2 \left[ \sum_{i=1}^{N_2} \frac{d^4 \varphi_{2i}(x_2)}{dx_2^4} q_{2i}(t) \right] \psi_{2m_2}(x_2) dx_2 \tag{C10}$$

$$RII_{m_24} = C_{E2} \left[ \sum_{i=1}^{N_2} \varphi_{2i}(x_{E2}) \frac{dq_{2i}(t)}{dt} - u_E(t) \right] \psi_{2m_2}(x_{E2}) \tag{C11}$$

$$RII_{m_25} = k_{E2} \left[ \sum_{i=1}^{N_2} \varphi_{2i}(x_{E2})q_{2i}(t) - u_E(t) \right] \psi_{2m_2}(x_{E2}) \tag{C12}$$

$$RII_{m_26} = kn_{E2} \left[ \sum_{i=1}^{N_2} \varphi_{2i}(x_{E2})q_{2i}(t) - u_E(t) \right]^3 \psi_{2m_2}(x_{E2}) \tag{C13}$$

**References**

1. Kang, K.H., Kim, K.J.: Modal properties of beams and plates on resilient supports with rotational and translational complex stiffness[J]. *J. Sound Vib.* **190**(2), 207–220 (1996)
2. Kim, H.K., Kim, M.S.: Vibration of beams with generally restrained boundary conditions using Fourier series[J]. *J. Sound Vib.* **245**(5), 771–784 (2001)
3. Li, W.L.: Free vibrations of beams with general boundary conditions[J]. *J. Sound Vib.* **237**(4), 709–725 (2000)
4. Li, W.L., Zhang, X.F., Du, J.T., Liu, Z.G.: An exact series solution for the transverse vibration of rectangular plates with general elastic boundary supports[J]. *J. Sound Vib.* **321**, 254–269 (2009)

5. Ye, T.G., Jin, G.Y., Ye, X.M., Wang, X.R.: A series solution for the vibrations of composite laminated deep curved beams with general boundaries[J]. *Compos. Struct.* **127**, 450–465 (2015)
6. Wang, Q.S., Shi, D.Y., Liang, Q.: Free vibration analysis of axially loaded laminated composite beams with generally boundary conditions by using a modified Fourier-Ritz approach[J]. *J. Compos. Mater.* **50**(15), 2111–2135 (2016)
7. Chen, Q., Du, J.T.: A Fourier series solution for the transverse vibration of rotating beams with elastic boundary supports[J]. *Appl. Acoust.* **155**, 1–15 (2019)
8. Wang, Y.H., Du, J.T., Cheng, L.: Power flow and structural intensity analyses of Acoustic Black Hole beams. *Mech. Syst. Signal Process.* **131**, 538–553 (2019)
9. Xu, D.S., Du, J.T., Zhao, Y.H.: Flexural vibration and power flow analyses of axially loaded beams with general boundary and non-uniform elastic foundations[J]. *Adv. Mech. Eng.* **12**(5), 1–14 (2020)
10. Xu, D.S., Du, J.T., Tian, C.: Vibration characteristics and power flow analyses of a ship propulsion shafting system with general support and thrust loading. *Shock Vib.* **2020**, 1–13 (2020)
11. Özhan, B.B., Pakdemirli, M.: A general solution procedure for the forced vibrations of a system with cubic nonlinearities: three-to-one internal resonances with external excitation. *J. Sound Vib.* **329**, 2603–2615 (2010)
12. Ghayesh, M.H., Kazemirad, S., Darabi, M.A.: A general solution procedure for vibrations of systems with cubic nonlinearities and nonlinear/time-dependent internal boundary conditions. *J. Sound Vib.* **330**, 5382–5400 (2011)
13. Ghayesh, M.H., Kazemirad, S., Reid, T.: Nonlinear vibrations and stability of parametrically excited systems with cubic nonlinearities and internal boundary conditions: a general solution procedure. *Appl. Math. Model.* **36**(7), 3299–3311 (2012)
14. Wang, Y.R., Fang, Z.W.: Vibrations in an elastic beam with nonlinear supports at both ends. *J. Appl. Mech. Tech. Phys.* **56**(2), 337–346 (2015)
15. Mao, X.Y., Ding, H., Chen, L.Q.: Vibration of flexible structures under nonlinear boundary conditions. *J. Appl. Mech.* **84**(11), 111006 (2017)
16. Tang, B., Brennan, M.J., Manconi, E.: On the use of the phase closure principle to calculate the natural frequencies of a rod or beam with nonlinear boundaries. *J. Sound Vib.* **433**, 461–475 (2018)
17. Ding, H., Zhu, M.H., Chen, L.Q.: Nonlinear vibration isolation of a viscoelastic beam. *Nonlinear Dyn.* **92**, 325–349 (2018)
18. Ding, H., Lu, Z.Q., Chen, L.Q.: Nonlinear isolation of transverse vibration of pre-pressure beams. *J. Sound Vib.* **442**, 738–751 (2019)
19. Ding, H., Chen, L.Q.: Nonlinear vibration of a slightly curved beam with quasi-zero-stiffness isolators. *Nonlinear Dyn.* **95**, 2367–2382 (2019)
20. Zhao, Y.H., Du, J.T.: Dynamic behavior of an axially loaded beam supported by a mass-spring system that is nonlinear. *Int. J. Struct. Stab. Dyn.* **2021**, 2150152 (2021)

21. Georgiades, F., Vakakis, A.F.: Dynamics of a linear beam with an attached local nonlinear energy sink. *Commun. Nonlinear Sci. Numer. Simul.* **12**, 643–651 (2007)
22. Ahmadabadi, Z.N., Khadem, S.E.: Nonlinear vibration control of a cantilever beam by a nonlinear energy sink. *Mech. Mach. Theory* **50**, 134–149 (2012)
23. Ahmadabadi, Z.N., Khadem, S.E.: Nonlinear vibration control and energy harvesting of a beam using a nonlinear energy sink and a piezoelectric device. *J. Sound Vib.* **333**, 4444–4457 (2014)
24. Kani, M., Khadem, S.E., Pashaei, M.H., Dardel, M.: Vibration control of a nonlinear beam with a nonlinear energy sink. *Nonlinear Dyn.* **83**, 1–22 (2015)
25. Parseh, M., Dardel, M., Ghasemi, M.H.: Investigating the robustness of nonlinear energy sink in steady state dynamics of linear beams with different boundary conditions. *Commun. Nonlinear Sci. Numer. Simul.* **29**, 50–71 (2015)
26. Kani, M., Khadem, S.E., Pashaei, M.H., Dardel, M.: Design and performance analysis of a nonlinear energy sink attached to a beam with different support conditions. *J. Mech. Eng. Sci.* **230**(4), 527–542 (2015)
27. Parseh, M., Dardel, M., Ghasemi, M.H., Pashaei, M.H.: Steady state dynamics of a non-linear beam coupled to a non-linear energy sink. *Int. J. Non-Linear Mech.* **79**, 48–65 (2016)
28. Chen, J.E., He, W., Zhang, W., Yao, M.H., Liu, J., Sun, M.: Vibration suppression and higher branch responses of beam with parallel nonlinear energy sinks. *Nonlinear Dyn.* **91**, 885–904 (2018)
29. Zhang, Y.W., Hou, S., Xu, K.F., Yang, T.Z., Chen, L.Q.: Forced vibration control of an axially moving beam with an attached nonlinear energy sink. *Acta Mech. Sol. Sin.* **30**, 674–682 (2017)
30. Zhang, Z., Ding, H., Zhang, Y.W., Chen, L.Q.: Vibration suppression of an elastic beam with boundary inerter-enhanced nonlinear energy sinks. *Acta Mech. Sol. Sin.* **37**(3), 387–401 (2021)
31. Oniszczuk, Z.: Free transverse vibrations of elastically connected simply supported double-beam complex system. *J. Sound Vib.* **232**(2), 387–403 (2000)
32. Gurgoze, M., Erdogan, G., Inceoglu, S.: Bending vibrations of beams coupled by a double spring-mass system. *J. Sound Vib.* **243**(2), 361–369 (2001)
33. Pajand, M.R., Hozhabrossadati, S.M.: Free vibration analysis of a double-beam system joined by a mass-spring device. *J. Vib. Control* **22**(13), 3004–3017 (2014)
34. Hilal, M.A.: Dynamic response of a double Euler-Bernoulli beam due to a moving constant load. *J. Sound Vib.* **297**, 477–491 (2006)
35. Li, J., Hua, H.X.: Spectral finite element analysis of elastically connected double-beam systems. *Finite Elem. Anal. Des.* **43**, 1155–1168 (2007)
36. Rosa, M.A.D., Lippiello, M.: Non-classical boundary conditions and DQM for double-beams. *Mech. Res. Commun.* **34**, 538–544 (2007)
37. Zhang, Y.Q., Lu, Y., Wang, S.L., Liu, X.: Vibration and buckling of a double-beam system under compressive axial loading. *J. Sound Vib.* **318**, 341–352 (2008)
38. Stojanovic, V., Kozic, P., Pavlovic, R., Janevski, G.: Effect of rotary inertia and shear on vibration and buckling of a double beam system under compressive axial loading. *Arch. Appl. Mech.* **81**, 1993–2005 (2011)
39. Kozic, P., Pavlovic, R., Karlicic, D.: The flexural vibration and buckling of the elastically connected parallel-beams with a Kerr-type layer in between. *Mech. Res. Commun.* **56**, 83–89 (2014)
40. Palmeri, A., Adhikari, S.: A Galerkin-type state-space approach for transverse vibrations of slender double-beam systems with viscoelastic inner layer. *J. Sound Vib.* **330**, 6372–6386 (2011)
41. Mao, Q.B.: Free vibration analysis of elastically connected multiple-beams by using the Adomian modified decomposition method. *J. Sound Vib.* **331**, 2532–2542 (2012)
42. Mao, Q.B.: Vibration and stability of a double-beam system interconnected by an elastic foundation under conservative and nonconservative axial forces. *Int. J. Mech. Sci.* **93**, 1–7 (2015)
43. Mohammadi, N., Nasirshoaibi, M.: Forced transverse vibration analysis of a Rayleigh double-beam system with a Pasternak middle layer subjected to compressive axial load. *J. Vibroeng.* **17**(8), 4545–4559 (2015)
44. Pisarski, D., Szmjdt, T., Bajec, C., Dyniewicz, B., Bajkowski, J.M.: Vibration control of double-beam system with multiple smart damping members. *Shock Vib.* **2016**, 1–14 (2016)
45. Fei, H., Danhui, D., Cheng, W., Jia, P.F.: Analysis on the dynamic characteristic of a tensioned double-beam system with a semi theoretical semi numerical method. *Compos. Struct.* **185**(1), 584–599 (2018)
46. O.O. Agboola, J.A. Gbadeyan, S.A. Iyase. Effects of some structural parameters on the vibration of a simply supported non-prismatic double-beam system. *Proceedings of the World Congress on Engineering, 2017, IWCE, Vol I, London, UK*
47. Rahman, M.S., Lee, Y.Y.: New modified multi-level residue harmonic balance method for solving nonlinearly vibrating double-beam problem. *J. Sound Vib.* **406**, 295–327 (2017)
48. Lee, J., Wang, S.Y.: Vibration analysis of a partially connected double-beam system with the transfer matrix method and identification of the slap phenomenon in the system. *Int. J. Appl. Mech.* **9**(7), 1750093 (2017)
49. Chen, L.J., Xu, D.S., Du, J.T., Zhong, C.W.: Flexural vibration analysis of nonuniform double-beam system with general boundary and coupling conditions. *Shock Vib.* **2018**, 1–8 (2018)
50. Hao, Q.J., Zhai, W.J., Chen, Z.B.: Free vibration of connected double-beam system with general boundary conditions by a modified Fourier-Ritz method. *Arch. Appl. Mech.* **88**, 741–754 (2018)
51. Zhao, X.Z., Asce, P.E.M.: Solution to vibrations of double-beam systems under general boundary conditions. *J. Eng. Mech.* **147**(10), 04021073 (2021)
52. Li, Y.X., Xiong, F., Xie, L.Z., Sun, L.Z.: State-space approach for transverse vibration of double-beam systems. *Int. J. Mech. Sci.* **189**, 105974 (2021)



53. Pajand, M.R., Sani, A.A., Hozhabrossadati, S.M.: Analyzing free vibration of a double-beam joined by a three-degree of freedom system. *J. Braz. Soc. Mech. Sci. Eng.* **41**, 211 (2019)
54. Guo, T.D., Kang, H.J., Wang, L.H., Zhao, Y.Y.: Nonlinear vibrations for double inclined cables–deck beam coupled system using asymptotic reductions. *Int. J. Non-Linear Mech.* **108**, 33–45 (2019)
55. Stojanovic, V., Petkovic, M.D., Milic, D.: Nonlinear vibrations of a coupled beam-arch bridge system. *J. Sound Vib.* **464**(4), 115000 (2020)

**Publisher's Note** Springer Nature remains neutral with regard to jurisdictional claims in published maps and institutional affiliations.

Springer Nature or its licensor (e.g. a society or other partner) holds exclusive rights to this article under a publishing agreement with the author(s) or other rightsholder(s); author self-archiving of the accepted manuscript version of this article is solely governed by the terms of such publishing agreement and applicable law.